INVITED PAPER

MATRIX METHODS OF AEROSPACE STRUCTURAL ANALYSIS

Paul H. Denke*

Douglas Aircraft Company, McDonnell Douglas Corporation

The future development of key areas in the field of matrix structural analysis is considered. The relationship of these areas to the overall design problem is established, and sources of past difficulties within the areas are identified. Avenues of approach to the difficulties are suggested and illustrated by reference to recently conducted research. In the area of modelling, the triangular membrane element and the bar-panel idealization are evaluated. A method of improving results obtained from the analysis of models composed of triangular membrane elements is presented. The loss of numerical accuracy in linear structural analysis is considered and methods of improving accuracy are described. Problems in the field of nonlinear structural analysis are reviewed. The possiblity of an interactive computational approach to the synthesis of comples structures is suggested, and an interactive graphics approach to the synthesis of a structure subjected to steady-state vibration is demonstrated.

*Director, Scientific Computing

Report Documentation Page

Form Approved
OMB No. 0704-0188

1. REPORT DATE	2. REPORT TYPE	3. DATES COVERED
OCT 1968		**00-00-1968 to 00-00-1968**

4. TITLE AND SUBTITLE	5a. CONTRACT NUMBER
Matrix Methods of Aerospace Structural Analysis	5b. GRANT NUMBER
	5c. PROGRAM ELEMENT NUMBER
6. AUTHOR(S)	5d. PROJECT NUMBER
	5e. TASK NUMBER
	5f. WORK UNIT NUMBER
7. PERFORMING ORGANIZATION NAME(S) AND ADDRESS(ES) **Air Force Flight Dynamics Laboratory,Wright Patterson AFB,OH,45433**	8. PERFORMING ORGANIZATION REPORT NUMBER
9. SPONSORING/MONITORING AGENCY NAME(S) AND ADDRESS(ES)	10. SPONSOR/MONITOR'S ACRONYM(S)
	11. SPONSOR/MONITOR'S REPORT NUMBER(S)

12. DISTRIBUTION/AVAILABILITY STATEMENT
Approved for public release; distribution unlimited

13. SUPPLEMENTARY NOTES
See also AD0703685, Proceedings of the Conference on Matrix Methods in Structural Mechanics (2nd) Held at Wright-Patterson Air Force Base, Ohio, on 15-17 October 1968.

14. ABSTRACT

15. SUBJECT TERMS

16. SECURITY CLASSIFICATION OF:			17. LIMITATION OF ABSTRACT	18. NUMBER OF PAGES	19a. NAME OF RESPONSIBLE PERSON
a. REPORT	b. ABSTRACT	c. THIS PAGE			
unclassified	**unclassified**	**unclassified**		**66**	

SECTION I

INTRODUCTION

In searching for a suitable theme for this opening paper, the writer was impressed with two features of the conference agenda that seem especially important. The first feature is that the field of interest is broad. We are not only interested in the ordinary behavior of structures subjected to loads well within the elastic range, but we are also concerned with the exceptional behavior resulting from the application of loads outside this range. We are interested in the application of matrix algebra to the analysis of structures, as well as the process of structural idealization that must precede analysis. We are interested in structural synthesis, which is the process of designing a structure to meet a given set of criteria. We are interested in dynamics as well as statics, and in the application to our problems of computing devices, such as graphics consoles. Finally, no restrictions are imposed on the intended purposes of the structures we consider. Many of our methods can apply equally well to aircraft, missiles, space vehicles, ships, submarines, buildings, and bridges.

A second important feature of the agenda is that the need for progress in the field is great. Designers must cope with ever more stringent requirements resulting from projects of an advanced nature, such as aircraft designed for vertical take-off, supersonic and hypersonic flight, and vehicles intended for lunar missions. In striving for structural integrity and efficiency the designer is not aided by spectacular breakthroughs, as in other fields. Whereas, the speed of flight has increased from about 300 miles per hour to orbital velocity in 30 years, a ratio of roughly fifty to one, the structural designer considers himself fortunate if the strength-to-weight ratios of his materials have increased by 50 percent in the same period of time.

Because the field is so broad, only certain key areas--where the need for accelerated progress seems most urgent--have been selected for discussion. The objective of this paper is to consider the future development of these key areas in order to:

- establish the significance of each area as related to the overall problem of structural design
- identify clearly the sources of past difficulties
- suggest some approaches to these difficulties
- illustrate certain approaches by reference to research recently conducted by the writer.

Engineers and scientists working in a highly technical field, such as structural analysis, often concentrate their efforts in specialized areas. It is hoped that this paper will serve to provide a useful overview of a significant fraction of the entire field, and that it will point the way to avenues of research that will prove useful in the future. These areas include discrete element idealization, linear structural analysis, nonlinear analysis, synthesis and the interactive application of remote graphics consoles to problems of steady-state vibration.

SECTION II

DISCRETE ELEMENT IDEALIZATIONS

This section is limited to a consideration of discrete idealizations, or models, composed of finite numbers of elements. These elements are connected at joints or nodes which also serve as application points for idealized discrete equivalents of actual external loads.

Two principal classes of models are defined. A displacement model is composed of elements having force-deformation characteristics such that continuity of displacements exists across element boundaries, while the characteristics of equilibrium models are such that continuity of stresses is maintained (Reference 1).

The present status of modelling can be summarized roughly as follows: Framed structures can be modelled without difficulty. Structural elements that represent plates, shells and solid bodies have been devised. These elements provide reliable results only if properly employed by experienced personnel. Better plate and shell elements, together with better methods of interpreting results derived from these elements, are needed. Better methods of evaluating the usefulness of elements are also desired.

METHODS OF ANALYSIS

A clear distinction should be made between the structural model and the method whereby the model is analyzed. Such a distinction is necessary to provide a proper basis for discussing the difficulties involved in the two areas.

The static behavior of a linear discrete structure is governed by equations of equilibrium and compatibility. Three methods of solving these equations are defined. In the Force Method, displacements are eliminated from the governing equations. The resulting equations are solved for element forces, which serve as the basis for calculating displacements. In the Displacement Method, element forces are eliminated from the governing equations. The resulting equations are solved for displacements. Elements forces are calculated from these displacements. In the Unified Method, the equations are solved in no predetermined order.

The Force and Displacement Methods are subsets of the Unified Method as demonstrated by Kosko (Reference 2). The definitions of these methods do not depend on the structural model. Any of the three methods, therefore, can be employed to analyze either displacement or equilibrium models. The results obtained through the use of any of the three methods are the same, except for loss of accuracy during computation, when applied to any particular model regardless of type, since the governing equations being solved in each case are the same.

The degree of accuracy inherent in a given model should not be attributed to a particular analysis method. For example, the statement that the Force Method gives upper bounds for deflection influence coefficients is, generally, not true.

MODELLING CRITERIA

An attempt to assess the usefulness of structural models must be based on criteria of some kind. Following are three criteria that seem to be generally accepted:

1. Convergence - As the sizes of elements in a model approach zero, the errors in computed stresses and deflections should approach zero. The convergence should be monotonic.

2. Rate of Convergence - The usefulness of an element is proportional to its rate of convergence.

3. Computational Efficiency - The usefulness of an element is proportional to the ratio of accuracy to computational effort.

INTERPRETATION

The stresses and deflections mentioned in the criteria are nominal values derived from the model according to some rule of interpretation. For example, nodal deflections are

normally interpreted to be structural deflections. Various options are open for stress interpretation. Thus, the stresses at the center of a membrane element can be interpreted as the stresses at the corresponding point of the structure. Some interpretation rule must be established before the modelling criteria can be applied.

MODEL EVALUATION

One method for evaluating discrete membrane elements is to consider a plane stress problem having a known solution. For example, a plate of a given shape is subjected to boundary stresses. A closed form solution for the resulting internal stress distribution is known. The plate is then idealized with, say, triangular elements of a certain size. Stresses and deflections are numerically computed and compared with the known solution. The process is repeated for elements of different sizes. Convergence is studied.

A METHOD OF DISCRETE ELEMENT EVALUATION

The following paragraphs describe a different approach to element evaluation. It is similar to the preceding approach, except that after the plate is modelled with discrete elements it is analyzed mathematically instead of numerically. Difference equations are written for stresses and deflections. These equations are solved and the results are compared with known solutions to provide expressions for stress and deflection errors as functions of panel size. This method has several advantages. First, a precise expression for rate of convergence is obtained. Conclusions about convergence are not obscured by errors that occur when stresses and deflections are numerically computed. Second, results are obtained for a continuous range of element sizes. Third, a study of the error expressions can lead to a better understanding of element behavior. As a consequence, methods of correcting the results or of improving the elements themselves can be devised. Fourth, the best rules for interpreting results can be established.

SECTION III

THE EQUILATERAL TRIANGULAR CONSTANT STRESS MEMBRANE ELEMENT, POISSON'S RATIO = 1/3

Figure 1 shows a triangular element applicable to the Matrix Force method. The forces F_1, F_2, and F_3 act parallel to the element edges. The corresponding deformations are edge elongations. Stresses in the element are assumed to be uniform. Appendix 1 describes the element in more detail.

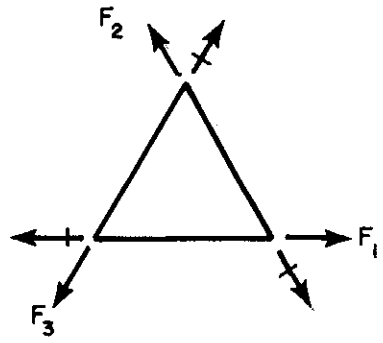

Figure 1. Triangular Membrane Element

LINEAR STRESS DISTRIBUTION, TRIANGULAR ELEMENTS

Appendix 1 presents a study of the behavior of the triangular element in a general linear stress field. The element is considered to be part of a grid of the kind shown in Figure 2, although the grid shape may vary. The grid is a model of an isotropic plate of uniform thickness. Loads act upon the boundaries distributed in such a manner that internal stresses are linear functions of the coordinates.

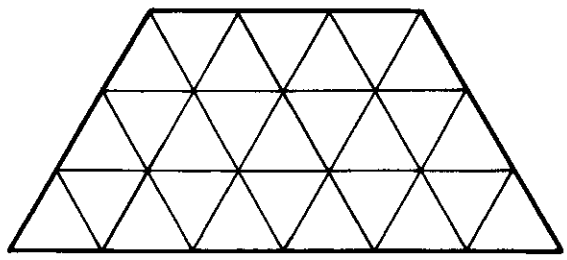

Figure 2. Idealized Plate

With these assumptions the analysis of the model is a simple matter. The true displacements of the plate are first calculated. These displacements are then applied to joints of the model and the resulting external loads are determined. Element forces and element stresses are computed. Appendix 1 contains the details of the analysis. The results follow. These results also apply to the uniformly stressed triangular element employed in the Matrix Displacement method.

Edge Loads

The analysis shows that normal and tangential loads applied to a joint on the edge of the idealized plate should be equal to the boundary normal and shear stresses, respectively, acting at the joint multiplied by the length of the edge of the element and the thinkness of the plate. No loads are applied to internal joints. The idealized plate is in equilibrium under these loads when the stress distribution is linear.

Deflections

The computed deflections are exact when the loads are applied as described in the preceding paragraph. Deflections of joints of the idealized structure should be interpreted as deflections at corresponding points of the plate.

Stresses

An attempt was made to find a point in each element of the model at which the computed uniform stresses in the element are equal to the true stresses at the corresponding point in the plate. No such point exists. Next, an attempt was made to find a point in each element at which the sum of the squares of the errors in the stresses is minimized. Discovery of such a point would provide a rule for stress interpretation. No single point was found. Instead the location of the optimum point was found to depend on the type of linear stress field acting on the plate.

Since no unique optimum point was found, a study was made of errors at the centroid of the triangle. The results are given by Equation (33) and are summarized as follows: First, the stress errors at the centroid of the element converge to zero as the length of the side of the element approaches zero. Second, the errors are proportional to the length of the side of the element and the stress distribution parameters b_1, b_2, b_3, and b_4. Third, the errors are independent of element location.

These results indicate that calculations based on the triangular element generally converge, as long as the stress field contains no singularities, because the field in the region of an element will tend to approach linearity as the element becomes smaller.

Percentage Error

The error in a quantity measured or calculated by some approximate procedure can be expressed as a percentage of the known correct value. This procedure is not applicable for present purposes because small errors in stresses that have very small or zero exact values produce large percentage errors which are misleading. The following procedure is adopted: Errors in tensile stress components are divided by an equivalent tensile stress, $\overline{\sigma}$, defined as the uniform tensile stress that would produce the same amount of strain energy in the plate as the actual stress distribution. Errors in shear stress components are likewise divided by an equivalent uniform shear stress, $\overline{\tau}$, defined in a similar manner. These reference stresses, which are constant for any particular loading condition, are derived as follows: The strain energy stored in a plate subjected to plane stress is:

$$W = \frac{1}{2}\frac{t}{E}\int_A \left[\sigma_x^2 + \sigma_y^2 - 2\nu\sigma_x\sigma_y + 2(1+\nu)\tau_{xy}^2\right] dA \qquad (1)$$

where t = plate thickness, E = Young's modulus, ν = Poisson's ratio and σ_x, σ_y, and τ_{xy} are components of the stress tensor. If $\sigma_x = \overline{\sigma}$ (constant) and $\sigma_y = \tau_{xy} = 0$, then

$$\overline{\sigma} = \sqrt{\frac{2E}{At}W}$$

If $\tau_{xy} = \overline{\tau}$ (constant) and $\sigma_x = \sigma_y = 0$, then

$$\overline{\tau} = \sqrt{\frac{EW}{A(1+\nu)}} = \frac{\overline{\sigma}}{\sqrt{2(1+\nu)}} \qquad (2)$$

Stress Correction Procedure for Constant Stress Triangular Elements

The notion of the stress field in the region of an element becoming approximately linear as the element decreases in size suggests a method of improving stresses computed from triangular elements. The method is based on the assumption that a linear stress field that approximates the computed stress distribution can be found in the region of an element. Appendix 2 contains the derivation of the method.

When the correction procedure is applied to the approximate stresses derived from the equilateral triangular grid subjected to a linear stress field, exact results are obtained. The method also produces excellent results in the following highly nonlinear case.

A concentrated load acts upon one vertex of the triangular plate shown in Figure 3.

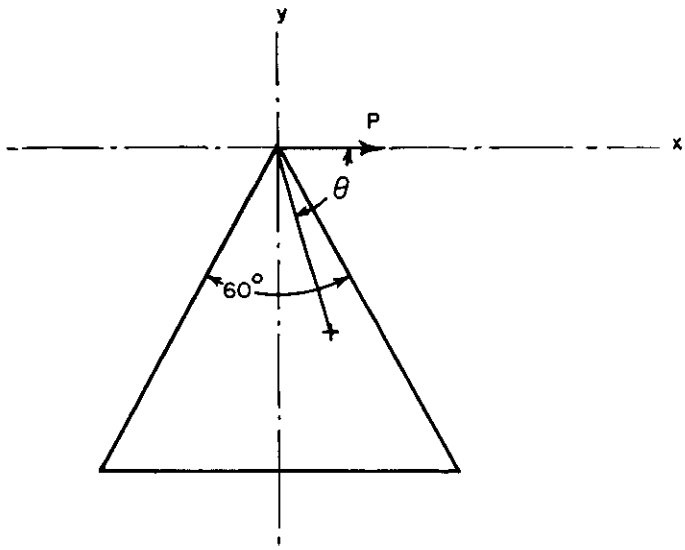

Figure 3. Loaded Triangular Plate

Equilibrium is produced by stresses acting along the lower edge. The following stresses and displacements of the plate are derived from Reference 4.

$$\left.\begin{aligned} \sigma_x &= \frac{-2kx^3}{(x^2+y^2)^2} \\ \sigma_y &= \frac{-2kxy^2}{(x^2+y^2)^2} \\ \tau_{xy} &= \frac{-2kx^2y}{(x^2+y^2)^2} \end{aligned}\right\} \tag{3}$$

$$\left.\begin{aligned} \frac{E}{k}u &= \frac{x^2-y^2/3}{x^2+y^2} - \ln\left(\frac{4}{3}\frac{x^2+y^2}{b^2}\right) - \left(\frac{2\pi}{9}+\frac{2\sqrt{3}}{3}\right)\frac{y}{b} - \frac{\pi\sqrt{3}}{9} - \frac{2}{3} \\ \frac{E}{k}v &= \frac{4}{3}\frac{xy}{x^2+y^2} + \frac{2}{3}\left(\frac{\pi}{2} - \tan^{-1}\frac{y}{x}\right) + \left(\frac{2\pi}{9}+\frac{2\sqrt{3}}{3}\right)\frac{x}{b} \end{aligned}\right\} \tag{4}$$

where

$$k = \frac{P}{\left(\frac{\pi}{3} - \frac{\sqrt{3}}{2}\right)t} \tag{5}$$

The plate was replaced by structural models composed of equilateral triangular membrane elements, and stresses computed from the models were compared with exact results and with stresses computed according to the correction procedure of Appendix 2. Three grid sizes were studied: fine, medium, and coarse. Figure 4 shows the medium fineness model. The fine grid had twice as many elements per edge and the coarse grid had half as many. The triangular

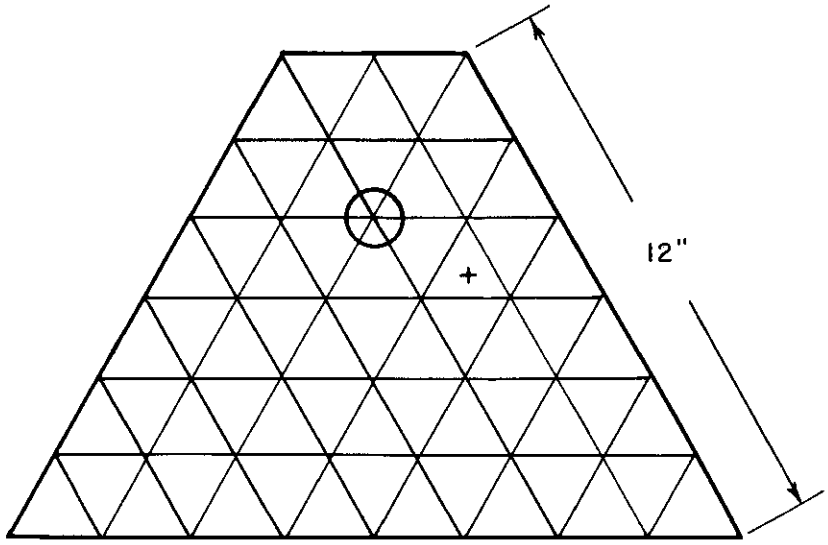

Figure 4. Medium Grid Model

plate was truncated as shown because the concentrated load applied at the vertex produces infinite stresses and deflections, at that point, which are not realistic.

Each model was analyzed in the following manner. Nodal displacements were accurately calculated from Equation 4. The matrix of displacements was multiplied by the assembled stiffness matrix to produce external loads. Element deformations were calculated from displacements, and element stress components (σ_x, σ_y, τ_{xy}) were computed from element deformations. The model was thus analyzed as a kinematically determinate structure. This procedure has three advantages compared to idealizing edge loads and computing deflections and stresses from these loads. First, the loss of accuracy involved in solving simultaneous equations is avoided. Second, the uncertainty resulting from idealizing edge loads according to some arbitrary rule is avoided. Third, a study of the computed external loads may suggest rules for load idealization. The kinematically determinate structure, although a somewhat unusual subject for study, should yield reliable information on convergence.

Figure 5 shows the convergence of external load at the node indicated by a circle in Figure 4. The error in the load acting at the node, expressed as a percentage of the load acting

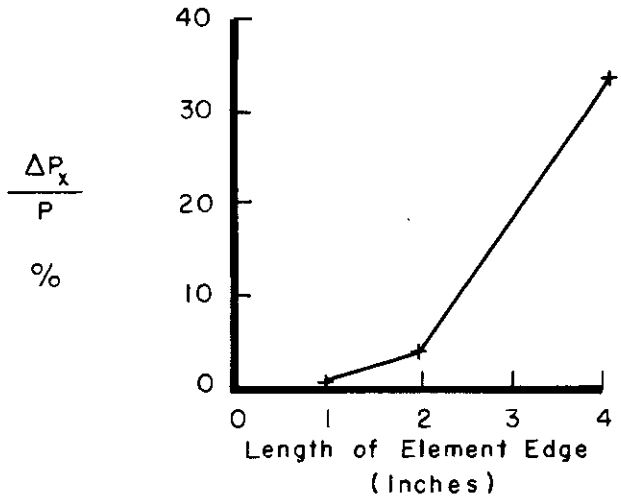

Figure 5. Convergence of Interior Joint Loads

at the vertex of the triangular plate, is plotted as a function of length of element edge. The load should be zero since the node is on the interior of the plate. Figure 5 indicates a satisfactory convergence.

Figure 6 shows the convergence of shear stress at the point indicated by a plus mark (+) in Figure 4. The shear stress error, as a percentage of the mean shear stress in the plate, is plotted as a function of length of element edge. The corrected shear stress shows a very satisfactory convergence.

The shear and normal loads acting at nodes on the upper and lower edges of the plate were found to approach the shear and normal stresses acting at these nodes multiplied by the length of the element edge and the thickness of the plate.

The results shown in Figures 5 and 6 are typical of the entire plate. The errors in the medium-grid-corrected stresses are on the order of three percent compared to about 20 percent for uncorrected stresses. The corresponding values for the fine grid are about one percent and nine percent.

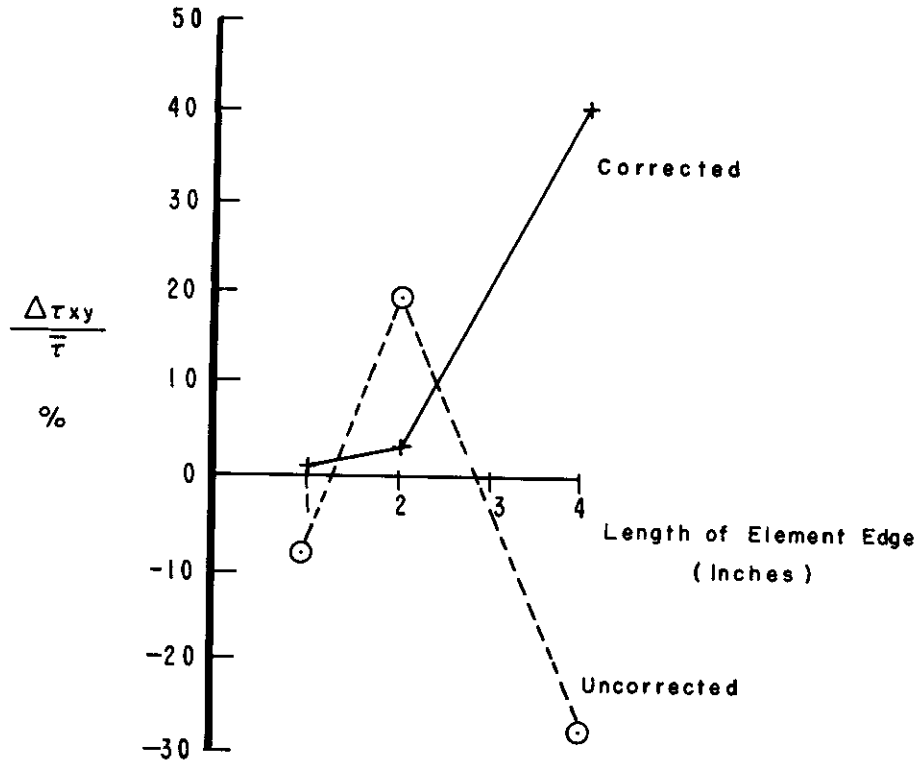

Figure 6. Convergence of Shear Stress

The equilateral triangular element, on the basis of convergence of external loads and corrected stresses, can be considered to meet the modelling criteria in a satisfactory manner. A good deal of confidence can be placed in the convergence of deflections when loads are specified, as a result of the satisfactory convergence of loads when deflections are specified. This conclusion holds, provided that excessive accuracy is not lost in the solution of simultaneous equations.

SECTION IV

THE RECTANGULAR BAR-PANEL IDEALIZATION

Figure 7 shows a bar-panel idealization of a plate. The model consists of axially loaded bars, and plate elements or panels that carry shear only. Panels are connected to bars at

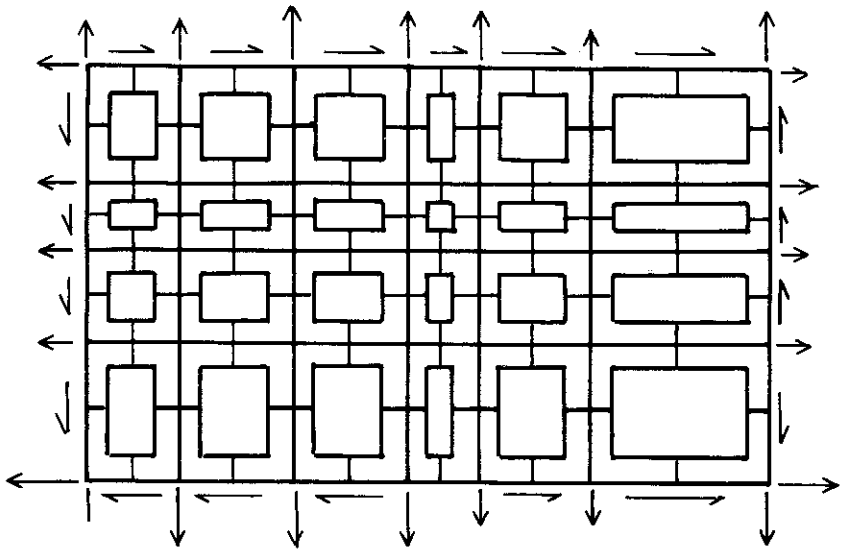

Figure 7. Bar-Panel Model

midpoints of panel edges. The point of connection between a panel and a bar is referred to in the following as a shear node. The point of intersection between two bars is called a joint. Normal edge loads act on joints, and tangential edge loads act on shear nodes. Bars need not be equally spaced. Bars and panels are constant stress elements.

LINEAR STRESS DISTRIBUTION, BAR-PANEL MODEL

The behavior of the bar-panel idealization in a linear stress field is analyzed in Appendix 3, accounting for Poisson's ratio and considering unequally spaced bars, with the following results:

Edge Loads

As in the case of triangular elements, the normal load applied to a joint should be equal to the boundary normal stress acting at the joint, multiplied by the distance between midpoints of adjacent panels and the plate thickness. The tangential load applied to the shear node should be equal to the boundary tangential stress at the node, multiplied by the length of the panel edge and the plate thickness.

Deflections

Deflections at joints are exact for the linear stress field when loads are applied as in the preceding paragraph. Deflections of shear nodes should be disregarded.

Stresses

Normal stresses in bars should be interpreted as normal stresses at points corresponding to joints in the plate. Shear stresses in panels should be interpreted as shear stresses at points corresponding to panel centers in the plate. Interpreted in this manner, the stresses produced by the bar-panel idealization are exact for the linear stress field.

QUADRATIC STRESS DISTRIBUTION, BAR-PANEL MODEL

The study of the behavior of the bar-panel model in the linear stress field throws no light on rate of convergence because stress and deflection errors are zero. The analysis of model behavior in a general quadratic stress field is therefore described in Appendix 3. Because of the complexity of this analysis, two simplifying assumptions are made. Bar elements are assumed to be equally spaced, and Poisson's ratio is assumed to be zero.

The stress function for the quadratic distribution involves four independent parameters d_1, d_2, d_4, and d_5. The effects of the distributions resulting from parameters d_5 and d_4 on the bar-panel model are essentially the same as the effects of the distributions resulting from d_1 and d_2, because of isotropy of the model. Only the distributions d_1 and d_2 need be considered. The results are as follows:

Edge Loads

For the d_1 distribution, edge loads should be idealized in the same manner as for the linear stress field. For the d_2 distribution this rule produces edge loads that do not satisfy equilibrium of moments. In Appendix 3 this moment imbalance is eliminated by a balancing couple uniformly distributed along the edges of the plate parallel to the Y-axis.

Deflections

The errors in joint deflections are proportional to the squares of lengths of panel edges.

Stresses

Errors in stresses for the d_1 distribution are zero. For the d_2 distribution, errors in tensile stresses are zero. The error in the shear stress is proportional to the square of the length of the panel edge parallel to the x-axis.

In order to derive quantitative results for the rate of convergence, consider the square plate shown in Figure 8 subjected to the quadratic stress field defined by putting $d_2 = 1$, $d_1 = d_4 = d_5 = 0$. From Equation 85 the stresses are $\sigma_x = 0$, $\sigma_y = 6xy$, $\tau_{xy} = -3x^2$. From Equations 2 and 85 the reference shear stress is

$$\bar{\tau} = \frac{1}{4}\sqrt{\frac{19}{5}}\, w^2 \tag{6}$$

From Equations 6 and 102 the absolute value of the percentage error is

$$\left|\frac{\Delta\tau_{xy}}{\bar{\tau}}\right| = \frac{0.512}{m^2} \tag{7}$$

where m is the number of shear elements per side of the plate. Figure 9 shows the convergence as a function of m.

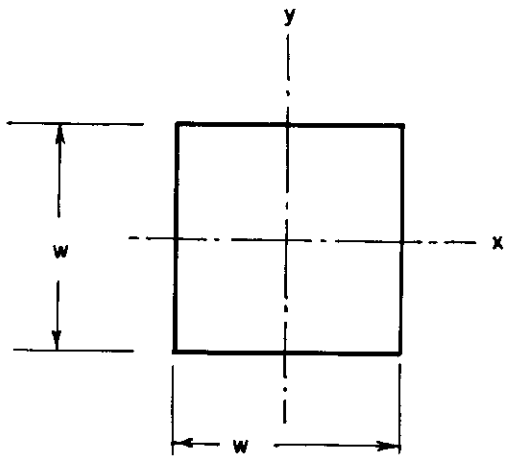

Figure 8. Square Plate

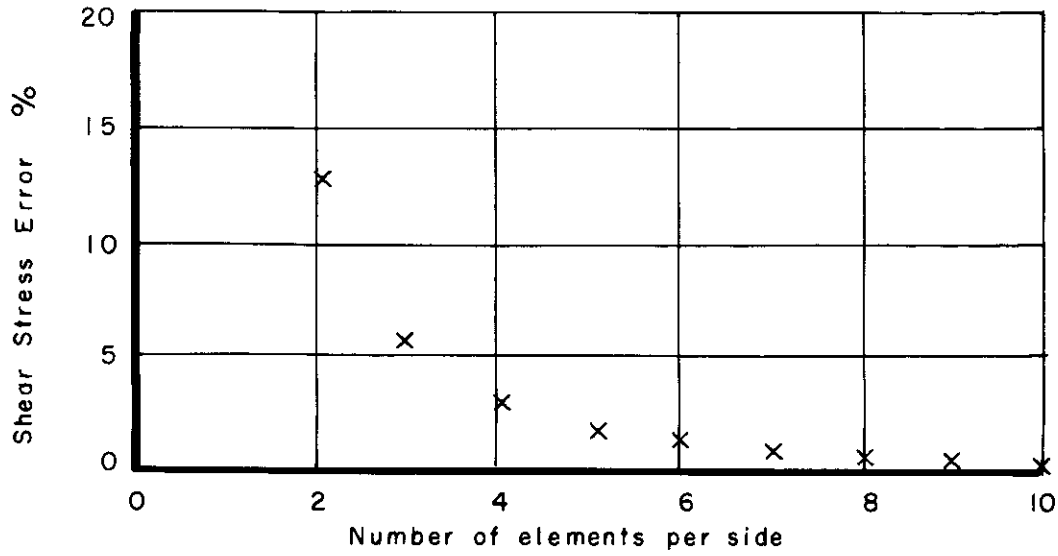

Figure 9. Convergence of Shear Stress in Bar-Panel Model

The bar-penel idealization can be considered to meet the modelling criteria in a satisfactory manner not only on the basis of the preceding analysis but also on the basis of many past comparisons with test results (Reference 11).

SECTION V

LINEAR STRUCTURES

The element force and displacement responses of structures in this category are linear functions of loads, support displacements, and unassembled element deformations.

BASIC APPROACHES TO STATIC ANALYSIS

The Force, Displacement, and Combined Methods differ in the order in which unknowns are computed, but all three methods provide solutions to the same governing equations. All three methods are applicable to any linear discrete model. The essential difference is in order of solution. This difference at first may not appear to be significant, but disputes concerning the comparative suitability of the three methods in various applications have persisted. A brief review of the pros and cons of this matter is offered.

Required Unknowns

If only deflections are required, the Displacement Method has an advantage because the effort needed to compute forces can be avoided. Similarly if only forces are required, the Force Method has an advantage.

Structural Model

The Displacement Method has an advantage when the model has a relatively low ratio of number of nodal displacements to number of redundants. The Force Method has an advantage when the ratio is high. The first situation tends to occur when the structure has many members in parallel, the second when the structure has many members in series. Particular types of elements seem better suited to one method than the other. For example, the rectangular constant stress membrane element seems better suited to the Displacement Method than the bar-panel idealization because the latter requires additional nodes at points where panels are joined to bars. Lumping (joining elements that serve parallel functions) is a useful procedure in the Force method for reducing the number of redundants.

Conditioning of the Governing Equations

Large complex structural models have a tendency to yield governing equations that are difficult to solve without significant loss of accuracy. The order of solution can be decisive

in successfully solving such equations. Forsyth has discussed this matter in some detail (Reference 5). As an example, consider the following matrix equation:

$$\begin{bmatrix} 1 & 0 & 0 & -1 & 0 \\ 0 & 10^{-6} & 0 & 1 & -1 \\ 0 & 0 & 1 & 0 & 1 \\ -1 & 1 & 0 & 0 & 0 \\ 0 & -1 & 1 & 0 & 0 \end{bmatrix} \begin{bmatrix} x_1 \\ x_2 \\ x_3 \\ x_4 \\ x_5 \end{bmatrix} = \begin{bmatrix} 0 \\ 0 \\ 0 \\ 0 \\ -1 \end{bmatrix} \tag{8}$$

A solution is sought on the basis of a Jordanian elimination process. The most straightforward approach is to attempt to eliminate the unknowns in the order x_1, x_2, x_3, x_4 to yield a solution for x_5, using diagonal elements as pivots. The following equation results after elimination of x_1, x_2 and x_3:

$$\begin{bmatrix} -1000001 & 1000000 \\ 1000000 & -1000001 \end{bmatrix} \begin{bmatrix} x_4 \\ x_5 \end{bmatrix} = \begin{bmatrix} 0 \\ -1 \end{bmatrix} \tag{9}$$

This equation is poorly conditioned. If a solution is attempted with a computer that carries less than seven significant decimal digits, the method fails.

If the unknowns are eliminated in the order x_5, x_4, x_1, x_3, x_2, with elements (3,5), (1,4), (4,1), (5,3) and (2,2) of the coefficient matrix as pivots, then the following results can be obtained with the aid of a two digit machine.

$$\{x_1 \quad x_2 \quad x_3 \quad x_4 \quad x_5\} = \{0.50 \quad 0.50 \quad -0.50 \quad 0.50 \quad 0.50\} \tag{10}$$

This result is a very good approximation to the exact solution which is

$$\{x_1 \quad x_2 \quad x_3 \quad x_4 \quad x_5\} = \frac{1}{2 + 10^{-6}} \{1, \ 1, \ -1 - 10^{-6}, \ 1, \ 1 + 10^{-6}\} \tag{11}$$

The scalar equations contained in Equation 8 are actually well-conditioned in the sense that an accurate solution can be obtained as a result of carrying a small number of significant digits, provided the order of solution is optimized. It seems worthwhile to distinguish between such equations and equations that are poorly conditioned. The term "order sensitive" is proposed to denote simultaneous equations having the property that solution accuracy is sensitive to order of elimination.

The example shows that some sets of equations are order sensitive. An approximate optimum order of solution can be discovered through the use of the procedure known as pivot selection (References 5 and 6). A suitable pivot selection strategy incorporated into equation solving routines for matrix structural analysis can significantly improve the accuracy of computed results.

The influence of order of elimination on solution accuracy has a bearing on the question of Force versus Displacement and Unified Methods. In the Unified Method no predetermined restrictions are placed on order of solution. The Unified Method in conjunction with pivot selection therefore provides in every case, a higher probability of success than either of the other two methods. Indications are that the governing equations are usually well conditioned, although order sensitive, if the structure is stable. The Unified Method with pivot selection should be a very reliable procedure. The principal disadvantage of the method is that all of the governing equations must be processed in one batch.

The other two methods involve prescribed orders of solution. No one has been able to show which order has the greatest potential for accuracy. However, it is known that a structural model with one or more very stiff members produces poorly conditioned Displacement Method equations unless certain nodal displacements are deleted, whereas, the Force Method equations are well-conditioned in such cases. The detrimental effect of stiff members plus the lack of suitable pivot selection procedures may be the cause of difficulties sometimes experienced with Displacement Method solutions.

The Force Method involves the difficulty of redundant selection. One approach to this problem is to base the selection on experience and intuition. This approach is virtually useless for most large structures. A second approach is to select redundants by comparison with a standarized model, or a model for which a mathematical analysis is available. This approach should be reliable when a suitable comparison model can be found. Many structures are too complex to be dealt with in this manner. A third approach to redundant selection is known as the Structure Cutter. This approach is based upon the application of pivot selection procedures to solve the equilibrium equations in terms of the redundants plus the application of column weighting factors proportional to member stiffnesses (Reference 6). This procedure eliminates the redundant selection problem by completely automating the selection process. The Structure Cutter has the additional advantage of optimizing the order of solution of the equilibrium and compatibility equations involved in the Force Method.

Experience with both the Force and Displacement Methods has led the writer to believe that the Force Method with optimized redundant selection tends to provide a greater degree of accuracy than the Displacement Method.

Computational Efficiency and Convenience

The influences upon computational efficiency of the configuration of the structural model and the particular unknowns to be calculated have been discussed. Computational efficiency is also dependent upon the design of the computer program and the skill of the programmer. Extremely efficient programs applicable to special classes of statically indeterminate structures have been devised. User convenience is a function of the degree of automation built into the program. Maximizing the degree of automation saves valuable engineering time and increases reliability. These comments apply equally to the Force and Displacement Methods.

PROGRAMMING SYSTEMS

A valid approach to developing an automated system of structural analysis is to write programs applicable to particular types of structures such as beams, plates, and shells of revolution. A second approach is to develop general purpose programs. This approach has proven feasible and worthwhile because many components of typical aircraft, missile, and space vehicle structures do not fall into recognizable categories. The following paragraphs describe a general purpose system recently developed at the Douglas Aircraft Company under sponsorship of the Air Force Flight Dynamics Laboratory.

FORMAT System

The FORTRAN Matrix Abstraction Technique (FORMAT) is a general purpose programming system for matrix structural analysis. Detailed documentation of FORMAT is contained in References 7, 8, and 9. A description of some applications of the system is given in Reference 10. The purpose here is to describe briefly the project objectives, the programming concepts, and the degree to which the objectives have been met.

The major criteria originally identified for FORMAT were generality, communicability, flexibility, universality, and efficiency (Reference 6). Generality meant that the program should be applicable to a broad range of structures. Communicability meant that the mathematical procedures should be formulated in such a manner as to be intelligible to engineers working in related fields. Flexibility meant that users who were expert in matrix structural analysis

would be able to alter procedures to meet changing requirements with no additional programming effort. Universality meant machine independence. Efficiency meant maximum output at minimum engineering and computing cost.

Some of these criteria tend to be contradictory and compromises are necessary. An effort was made to optimize the overall effectiveness of the program.

The FORMAT system is programmed in three phases. Phase I generates matrices from raw data. The output of Phase I includes matrices required for the following functions: analysis of structures subjected to thermomechanical loading, analysis of symmetric structures, element modification, substructure joining, and analysis of elastic stability and undamped vibration. The phase also generates joint coordinates of some commonly used structural shapes, and maintains and updates files of data.

Phase II performs matrix operations according to abstraction instructions written by the user. A typical instruction is FXO = FX. MULT. XO, which means that matrix FXO is equal to FX postmultiplied by XO. The user thus has freedom in determining the sequence of operations. The program processes abstraction instructions, prints diagnostics, allocates matrices to available tapes in an optimized manner, and executes instructions. Matrices up to order 2000 can be processed.

Phase III prints Force and Displacement Method reports and provides a graphical output capability.

The original criteria for the system have essentially been met. The Displacement and Force method generators provide a selection of displacement and equilibrium elements sufficient to represent a broad range of engineering structures. The matrix notation and extensive user and programming documentation provide communicability. The matrix abstraction language provides flexibility. The machine independence provided by the FORTRAN coding is such that the program has been successfully run on a number of machine configurations, including the IBM 7094, IBM 7044-7094 direct couple, UNIVAC 1108, GE 635, and IBM 360/65. Some degree of computing efficiency was sacrificed to meet the other criteria, but the savings in programming effort and maintenance resulting from generality, flexibility, and relative machine independence are considered to more than offset possible increases in computing cost.

SECTION VI

NONLINEAR STRUCTURES

The governing equations for structures in this category are nonlinear in the unknown displacements and element forces. The nonlinearities result from any form of behavior that does not accord with the assumptions of small deflections and linear elasticity. In the presence of creep, responses to static loads are time-dependent. The search for solutions to nonlinear structural problems involves certain difficulties.

BASIC LAWS

The first difficulty is that the basic laws of material behavior are not completely known. The strain components of an incremental volume of material are functions of stress components, past histories of these components, and histories of other environmental factors such as temperature. The laws of macroscopic material behavior are probably different for each alloy.

REPETITIVE SOLUTIONS

The quadratic, cubic, and biquadratic equations in a single variable are the only nonlinear equations having closed form solutions. All other nonlinear equations, including the governing simultaneous equations for nonlinear structures, must be solved by repetitive processes. These processes are usually iterative or stepwise applications of linear approximations.

In the iterative approach, a solution is sought for a particular set of values of the independent variables. Various structural parameters, such as element stiffnesses, are functions of dependent variables, such as stress, which are unknown. Values of the parameters are assumed. Approximate dependent variables are calculated and revised parameters are determined on the basis of the new independent variables. The process is repeated until values of the unknowns are obtained that satisfy all of the governing equations to the required degree of accuracy.

In the stepwise approach the response is assumed to be linear over small increments of the independent variable, which can be load or time. The structural parameters existing at the beginning of the interval are assumed to apply to the entire interval. Various refinements of the technique exist. The iterative and stepwise approaches can be combined.

In both the iterative and stepwise approaches convergence is important. The results must converge to fixed values as the number of iterations increases, or as the size of steps in the stepwise method decreases. Convergence can be deceptive. The results can appear to converge without being even approximately correct. The process can be very slowly convergent or divergent. The results of the stepwise process can have properties which are characteristics of the method of solution rather than of the structure.

MULTIPLE ROOTS

The possession of multiple roots is a property of nonlinear equations. For a given set of loads several different sets of structural responses can satisfy the governing equations. Only one response is appropriate to the prior history of loading. The iterative approach converges on roots that depend upon the choice of the initial approximation and the method of solution. The stepwise approach has the advantage of reproducing the actual loading history and consequently has the potential capability of always converging on the correct set of roots.

NONVALIDITY OF SUPERPOSITION

A third difficulty is that the responses of a nonlinear structure to two separate loading conditions cannot be added to produce the response to the sum of the two conditions. The solution for each condition must be separately computed. The unit load approach as a labor saving device for developing responses to actual loading conditions is not applicable.

COMPUTING EFFORT

A fourth difficulty is that the magnitude of the computing task is very significantly increased for nonlinear structures as a result of the required repetitive approach and the inapplicability of superposition.

APPROACHES TO THE DIFFICULTIES

One possible means of remedying the lack of information on material behavior is to continue study of the subject on the molecular and crystalline levels. The forces that govern the behavior of these bodies may be simpler to classify and describe than the behavior of macroscopic bodies such as tensile coupons.

A second approach is to continue deliberate efforts to establish categories of idealized material behavior that are useful in structural analysis. Categories already established include nonlinear elasticity, perfect platicity and various time-dependent stress-strain laws. The criterion here is not how closely natural behavior is approximated, but the usefulness of the approximation.

The need for repetitive solutions, the existence of multiple roots and the inapplicability of superposition are fundamental and unavoidable. The impact of these difficulties can be diminished by searching for optimum methods of solution that minimize computing effort and maximize the probability of converging on the correct set of roots.

The irreducible minimum amount of calculation unfortunately can be expected to be at least an order of magnitude greater than the effort required for the linear case, which already has a reputation as a formidable computing task. A requirement therefore exists for vastly improved computing capability. Perhaps this improvement can be realized by developing specialized computers for the solution of nonlinear simultaneous equations. The requirements in the field of structural analysis may be sufficient to justify such development.

Finally, a need exists to define carefully the objectives of nonlinear structural analysis in view of the difficulties involved. The basic objective for airframe and space vehicle design is to find methods that are useful for design purposes, not to model nature in great detail.

SECTION VII

STRUCTURAL SYNTHESIS

Structural synthesis is the procedure of designing a structure to meet a criterion of merit within constraints. For example, a structure can be designed to have minimum weight (the criterion of merit), and to have the capability of supporting multiple loading conditions in such a manner that stresses and deflections do not exceed allowable values (the constraints).

Minimum weight is often employed as a criterion of merit. Maximum cost effectiveness is usually a more realistic criterion although more difficult to apply.

Some examples of constraints are as follows:

- No structural element shall fail by fracture or buckling at ultimate load
- No yielding shall occur at limit load
- No general instability shall occur
- Deflections must not exceed allowable values
- Aeroelastic effects (e.g., loss of aileron effectiveness) shall not exceed allowables
- No flutter shall occur
- No fatigue failure shall occur during the design life.

A list two or three times as long can easily be prepared. These constraints are important design requirements that must be satisfied.

The independent variables of the problem include loads and thermal environment. The unknown dependent variables include structural concept, structural geometry, member sizes, materials, means of attachment, and thermal protection.

NONLINEARITY OF THE SYNTHESIS PROBLEM

Figure 10 shows a simple pin-jointed statically indeterminate truss. The problem is to determine the member cross-sectional areas A_1, A_2, and A_3 in such a manner as to minimize weight, subject to the constraints that no member shall have a negative area. The loading

conditions are as follows: in condition 1, $\phi_1 = 1, \phi_2 = 0$; in condition 2, $\phi_1 = 0$, $\phi_2 = 1$. All members have the same allowable tensile stress σ_a. The stress-strain relationships are linear to failure. The material density is unity.

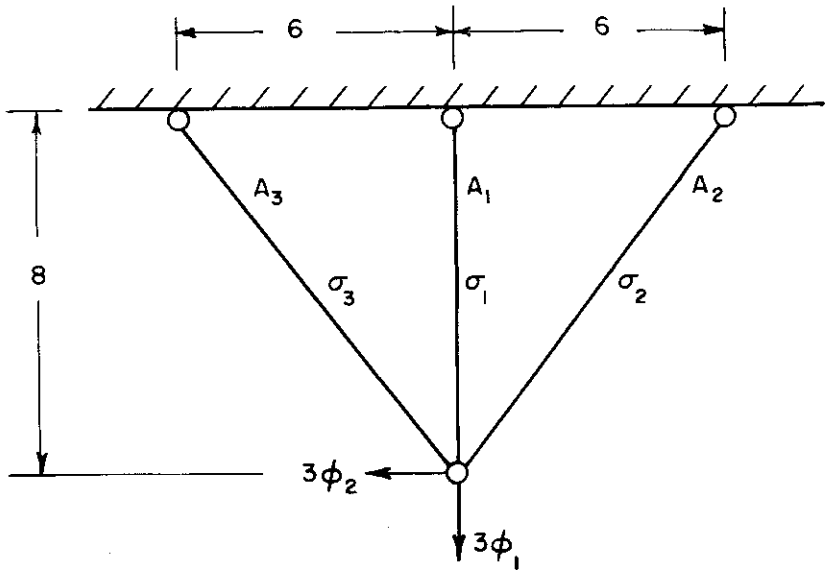

Figure 10. Statically Indeterminate Truss

Analysis of the problem yields the following relationships,
for Condition 1:

$$\left.\begin{aligned} \sigma_a\,(20.48\,A_2A_3 + 10\,A_3A_1 + 10\,A_1A_2) &\geq (30\,A_2 + 30\,A_3)\,\phi_1 \\ \sigma_a\,(20.48\,A_2A_3 + 10\,A_3A_1 + 10\,A_1A_2) &\geq 38.4\,A_3\phi_1 \\ \sigma_a\,(20.48\,A_2A_3 + 10\,A_3A_1 + 10\,A_1A_2) &\geq 38.4\,A_2\phi_1 \end{aligned}\right\} \qquad (12)$$

for condition 2:

$$\left.\begin{aligned} \sigma_a\,(20.48\,A_2A_3 + 10\,A_3A_1 + 10\,A_1A_2) &\geq (40A_3 - 40\,A_2)\,\phi_2 \\ \sigma_a\,(20.48\,A_2A_3 + 10\,A_3A_1 + 10\,A_1A_2) &\geq (51.2\,A_3 + 50\,A_1)\,\phi_2 \\ \sigma_a\,(20.48\,A_2A_3 + 10\,A_3A_1 + 10\,A_1A_2) &\geq (51.2\,A_2 + 50\,A_1)\,\phi_2 \\ \text{Also } A_1 \geq 0 \quad A_2 &\geq 0. \end{aligned}\right\} \qquad (13)$$

The mathematical formulation is in terms of inequalities rather than equations. These inequalitites are quadratic in the unknowns A_1, A_2 and A_3, even though the structure is linear. As more structural elements are added, the formulation of the synthesis problem becomes more highly nonlinear (not merely quadratic) and extremely complex.

NATURE OF SYNTHESIS

The general synthesis problem, which is the problem designers must solve, is formidable when stated in mathematical terms. The following complexities are involved: First, realistic criteria of merit, such as maximum cost effectiveness, are not easy to define with precision. Second, the list of constraints is very long. Third, the number of variables to be considered is large. Fourth, the problem is nonlinear. Fifth, the mathematical formulation tends to produce inequalities rather than equations. Finally, the synthesis problem includes all analytic problems, such as linear stress and deflection analysis, plasticity, buckling, and vibration. The mathematical formulation of the general synthesis problem is many orders of magnitude more complex than the most difficult problem in the field of structural analysis. The possibility of producing a general computer program for structural synthesis seems extremely remote.

APPROACH TO SYNTHESIS

Subsets of the general problem have been studied. Working computer programs have been developed (References 12 and 13) These programs are useful tools and they are significant advances in the state of the art. They contribute to the solution of the general problem but they do not solve it, yet this problem must be and is being solved daily to some degree of approximation. Two questions suggest themselves: First, how is the problem currently being handled? Second, how can the capability of the computer and the methods of matrix analysis be more efficiently applied to structural synthesis?

Obviously the answer to the first question is that the designer does the best he can with the tools he has. These tools include digital computers and computer programs, but the designer's most valuable aid is the ability to think creatively about the problem. The computer is entirely lacking in this ability which the human brain has in abundance. Even before the invention of the slide rule men were able to do a creditable job of structural design aided solely by computations performed with pencil on paper. On the other hand, the computer is far superior to man in the area of complex arithmetic calculation.

Recognition of this complementary relationship between man and machine led to the concept of Computer Aided Design (CAD) (References 14 and 15). According to this concept man and computer are placed in close contact, so that interaction time is minimized and maximum benefits are gained from the combination of abilities. The concept is implemented through the use of remote consoles, especially graphic consoles, connected to large computers provided with operating systems that allow the user almost instant response.

The idea of applying CAD principles to synthesis of complex structures is worth consideration in view of the difficulties of developing a completely automated system. Unfortunately many computing tasks associated with matrix structural analysis are too large for the interactive approach. On the other hand, some tasks can be approached in this manner. Such an application is described in the next section.

SECTION VIII

AN INTERACTIVE APPROACH TO STEADY STATE VIBRATION

Voluminous output tends to be characteristic of matrix structural analysis. Various means such as tables of maxima and minima are employed to reduce the amount of data the user must examine. Computer graphics provides an extremely effective means of condensing output. In a recent dynamic response study (16) an interactive graphics console displayed a moving picture of a vibrating structure. Such an application is especially useful because the dynamic display conveys an impression of mode shapes that cannot be easily gained from inspecting printed data.

The following paragraphs describe another application of the graphics console to structural vibration.

In this application, the steady state responses of a damped structure to oscillating inputs were studied. As a result the matrix formulations presented in Appendix 4 were developed. These formulations, which are generalizations of the Displacement, Force, and Unified Methods of static analysis, yield rigorous solutions to the equations of motion. The formulations are applicable to linear discrete structures. Each structural element has its own elastic and damping constants. Masses are attached to structural joints. All kinds of support and zero support are considered. Forcing functions that are sinusoidal functions of time of a single frequency but differing phases are applied. These forcing functions are external loads, support displacements, and unassembled element deformations. The unassembled deformations provide the basis for rapid computation of structural changes. Equations are given for time-dependent force and displacement responses of the structure.

In static analysis the effects of changing a structural element can be simulated by introducing into the element fictitious unassembled deformations. The magnitudes of these deformations are such that the assembled forces and deformations of the modified element are the same as they would be if the element stiffness actually were changed. This idea has been adapted to the analysis of vibrating structures. The resulting procedure for calculating modified response involves much less effort than computing the effects of a change from basic data.

The computations take place in two steps. The first step takes place in the batch mode. In this step the response of the original structure is calculated. In addition certain matrices are computed which are required in the second step as a basis for computing the effects of structural changes.

In the second step the user inputs through the graphics console the identification of the elastic element, mass, or damper he wishes to modify. He also inputs the factor by which he wishes to multiply the stiffness, the mass, or the damping constant. Changes to the deflection response are calculated and displayed. The user can modify the elements in any order by any amount. The same element can be modified repeatedly.

Figure 11 shows a structure consisting of a horizontal gridwork of beams and a number of vertical axially loaded members, as displayed on the face of the cathode ray tube. A mass is attached to each node, and an oscillating force of a given frequency acts at the upper end of the center vertical bar. Each element has its own damping constant.

Figure 12 shows the vibrating structure at a particular instant of time. A moving picture also can be displayed. The display can be rotated about each of the coordinate axes, and slices of the structure can be displayed for improved visibility.

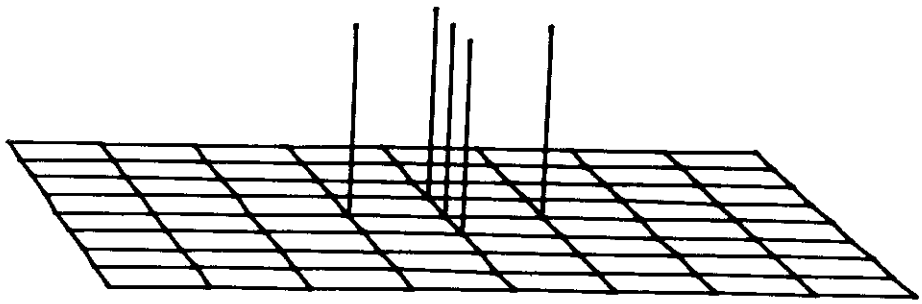

Figure 11. A Damped Elastic Structure

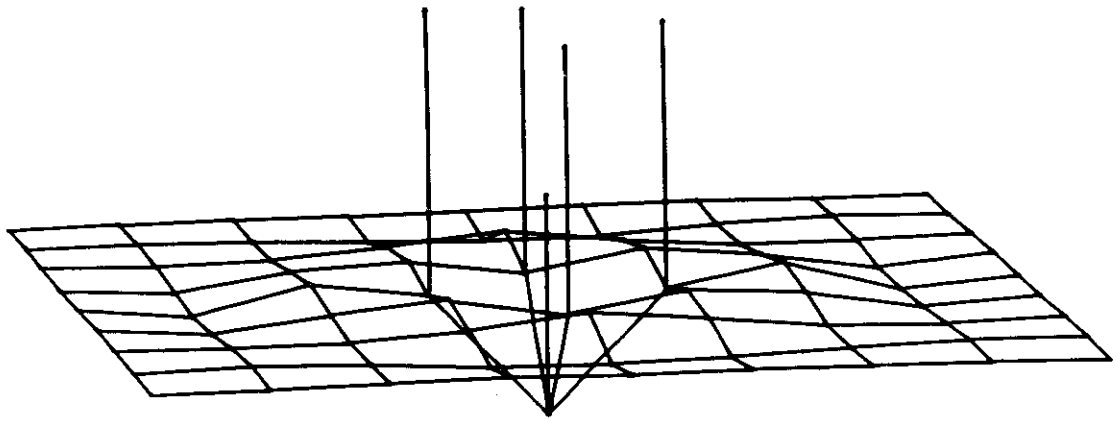

Figure 12. Response of a Damped Elastic Structure

Figure 13 shows the list of elements that are available for modification. The tables show the original value and the latest value of the modified element parameters. When the user requests a change to a structural element, 1-1/2 minutes are required for the machine to compute and display the revised deflection pattern. The modification program is thus a true interactive application of the graphics console to matrix structural analysis.

ELEMENT TYPE	SEQ. NO.	ELEM. NO.	ORIGINAL VALUE	SCALING FACTOR	LAST VALUE
ELASTIC	1	1	.17500E 04	.10000E 01	.17500E 04
ELASTIC	2	2	.17500E 04	.10000E 01	.17500E 04
ELASTIC	3	3	.17500E 04	.10000E 01	.17500E 04
ELASTIC	4	4	.17500E 04	.10000E 01	.17500E 04
ELASTIC	5	5	.17500E 04	.10000E 01	.17500E 04
MASS	6	87	.33333E 00	.10000E 01	.33333E 00
MASS	7	88	.33333E 00	.10000E 01	.33333E 00
MASS	8	89	.33333E 00	.10000E 01	.33333E 00
MASS	9	90	.33333E 00	.10000E 01	.33333E 00
MASS	10	91	.33333E 00	.10000E 01	.33333E 00
DAMPING	11	92	.17500E 04	.10000E 01	.61250E 04
DAMPING	12	93	.61250E 04	.10000E 01	.61250E 04
DAMPING	13	94	.61250E 04	.10000E 01	.61250E 04
DAMPING	14	95	.61250E 04	.10000E 01	.61250E 04
DAMPING	15	96	.61250E 04	.10000E 01	.61250E 04

SEQ. NO.	ORIGINAL VALUE	LAST VALUE	SCALING FACTOR	NEW VALUE
1	.17500E 04	.17500E 04	100.0_	

Figure 13. Modified Element Parameters

SECTION IX

SUMMARY

The field of structural modeling can benefit from the establishment of generally accepted criteria for discrete elements, and systematic methods of element evaluation. The evaluation methods should be as free as possible from the influences of extraneous factors, such as loss of accuracy in the process of numerical evaluation. An analytic evaluation avoids this difficulty and provides a better understanding of element behavior.

Loss of accuracy in solving the governing structural equations has always been a problem. The accuracy obtained in solving the equations by an elimination process can be sensitive to the order of elimination even when the equations are well conditioned. Accuracy can be improved by exercising care in establishing the elimination order and by employing a pivot selection technique during elimination.

The analysis of nonlinear structures involves the difficulties of repetitive solution, multiple roots, and nonvalidity of superposition. These difficulties significantly increase the scope of the computing task. Methods that minimize this task are needed. Development of specialized computing devices for solving nonlinear simultaneous equations may be justified for this and other applications.

The scope of the computing task involved in structural synthesis can be very large because a single synthesis can require the solution of many different kinds of analytic problems, such as stress analysis, stability, vibration, and fatigue. The task can be performed most efficiently through a combination of the creative powers of the analyst and the arithmetic and logical capability of the computer. A suitable combination can be effected by means of interactive graphics terminals and other devices that bring the user into close contact with the computer. Such an approach to the synthesis of complex structures should be considered. An interactive application of the remote graphics console to damped steady state structural vibration was demonstrated.

Acknowledgment

The study of convergence of results derived from models composed of triangular plate elements was performed with the aid of a computer program developed by S. Miyawaki at the Douglas Aircraft Company. The computer program and the graphics display program described in the section on structural vibration were developed by Miyawaki and K. Yankelevitz. These programs are based on analysis described in the body of the paper.

Work described in this paper was sponsored, in part, by the Air Force Flight Dynamics Laboratory, Air Force Systems Command, USAF, under USAF Contract No. F33615-67-C-1258. Additional information was developed by the Douglas Aircraft Company of the McDonnell Douglas Corporation as part of its Company sponsored Independent Research and Development programs.

SECTION X

REFERENCES

1. de Veubeke, B. F., Bending and Stretching of Plates, Special Models for Upper and Lower Bounds, AFFDL-TR-66-80, pp 863-886, 1965.

2. Kosko, E., The Equivalence of Force and Displacement Methods in the Matrix Analysis of Elastic Structures, AFFDL-TR-66-80, pp 329-351, 1965.

3. Przemieniecki, J. S., "Triangular Plate Elements in the Matrix Force Method of Structural Analysis," AIAA Journal, Volume 1, No. 8, pp 1895-1897, 1963.

4. Timoshenko, S., Theory of Elasticity, McGraw-Hill Book Company, Inc., New York, London, 1934.

5. Forsythe, G. E., "Today's Computational Methods of Linear Algebra," SIAM Review, Vol. 9, No. 3, pp 489-515, July 1967.

6. Denke, P. H., "Engineering Aspects and Mathematical Formulations of the Problem of a Computerized Aircraft Structural Analysis System," SAE Transactions No. 650055.

7. Bennett, D. K., et al., FORMAT I - First Version of Fortran Matrix Abstraction Technique, AFFDL-TR-65-47, 1965.

8. Pickard, J., Cogan, J. P. Jr., Lackey, W. J., Morris, R. C., and Serpanos, J. E., FORMAT II - Second Version of Fortran Matrix Abstraction Technique, AFFDL-TR-66-207, Vols. I-IV, 1967.

9. Pickard, J., Cogan, J. P. Jr., Morris, R. C., Wells, J. R., Yoon, P., and Lackey, W. J., FORMAT - Fortran Matrix Abstraction Technique, AFFDL-TR-66-207, Vols. V-VII, and Vol. II Supplement I, 1968.

10. Warren, D. S., "Applications Experience with the FORMAT Computer Program," Proceedings of the 2nd Conference on Matrix Methods in Structural Mechanics, October, 1968.

11. Denke, P. H., A General Digital Computer Analysis of Statically Indeterminate Structures, NASA TN D-1666, 1962.

REFERENCES (CONTD)

12. Gellatly, R. A., and Gallagher, R. H., "Development of Advanced Structural Optimization Programs and Their Application to Large Order Systems," AFFDL-TR-66-80, pp 231-251, 1965.

13. Fox, R. L. and Schmit, L. A., "An Integrated Approach to Synthesis and Analysis," Summer Course on Structural Synthesis, Case Institute of Technology, July, 1965.

14. Mann, R. W., "Engineering Specifications for a Man-Computer System for Design," M.I.T. Summer Session Course, Computer Aided Design, August, 1966.

15. Coons, S. A., "An Outline of the Requirements for a Computer Aided Design System," AFIPS Conference Proceedings, Volume 23, 1963 Spring Joint Computer Conference, pp 229-304.

16. Eshelman, A. L., and Meriwether, H. D., "Animated Display of Dynamic Characteristics of Complex Structures," Douglas Paper 4233, 1966.

APPENDIX I

EVALUATION OF THE EQUILATERAL TRIANGULAR CONSTANT STRESS ELEMENT, POISSON'S RATIO = 1/3

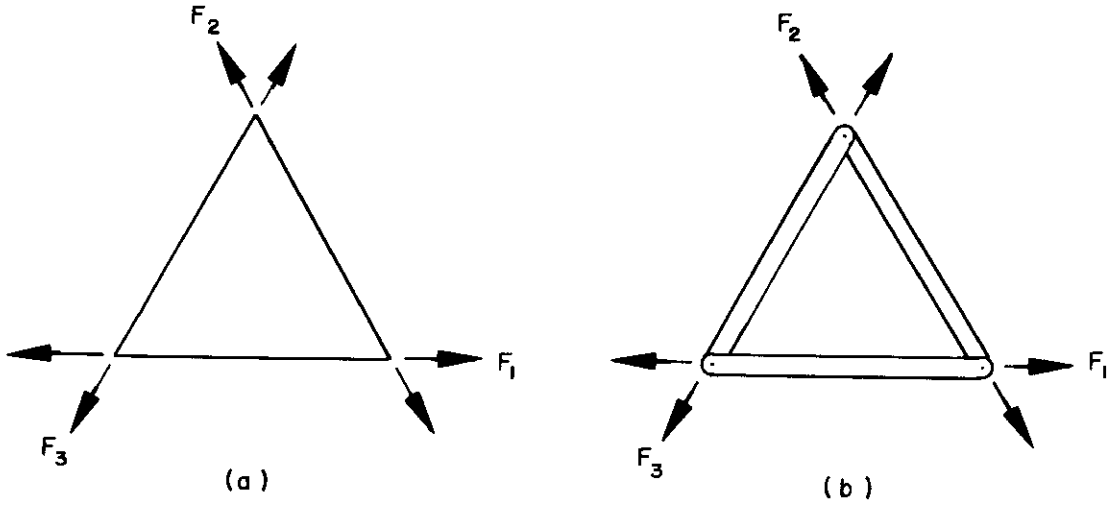

Figure 14. Equilateral Triangular Element

The flexibility matrix for the triangular element shown in Figure 14(a) is

$$D = \frac{1}{Et} \begin{bmatrix} \frac{4}{\sqrt{3}} & & \\ & \frac{4}{\sqrt{3}} & \\ & & \frac{4}{\sqrt{3}} \end{bmatrix} \tag{14}$$

where E is Young's modulus and t is the plate thickness.

Figure 14(b) shows a triangular frame composed of axially loaded bars of cross-sectional area $\sqrt{3}\,at/4$, where a is the length of the edge of the element.

The flexibility matrix for the frame is also given by Equation 14, consequently the equilateral triangle can be replaced by the framework of axially loaded bars. This substitution simplifies the discussion.

Difference Equations for a Model Composed of Equilateral Triangular Elements

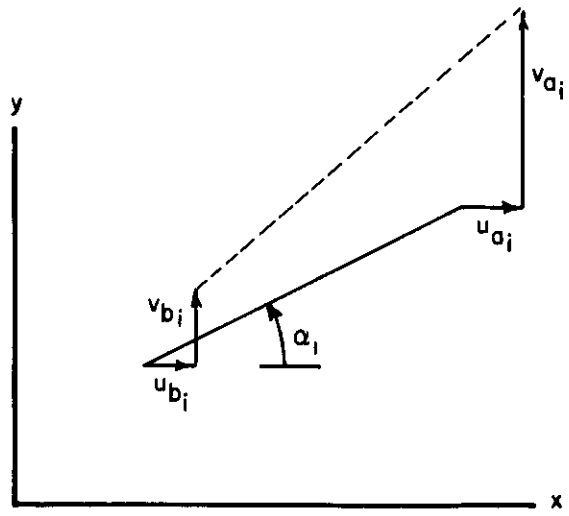

Figure 15. Displaced Bar

Figure 15 shows a bar of the triangular frame. The symbols for horizontal and vertical displacements of the ends of the bar are as shown. The subscript i indicates that the bar is the ith element of the grid. The deformation of the bar is

$$e_i = (u_{b_i} - u_{a_i}) \cos \alpha_i + (v_{b_i} - v_{a_i}) \sin \alpha_i \qquad (15)$$

where α_i is the angle between the bar and the X axis.

The element force in the bar is given in terms of the element deformation by

$$F_i = \frac{\sqrt{3}}{4} E t e_i \qquad (16)$$

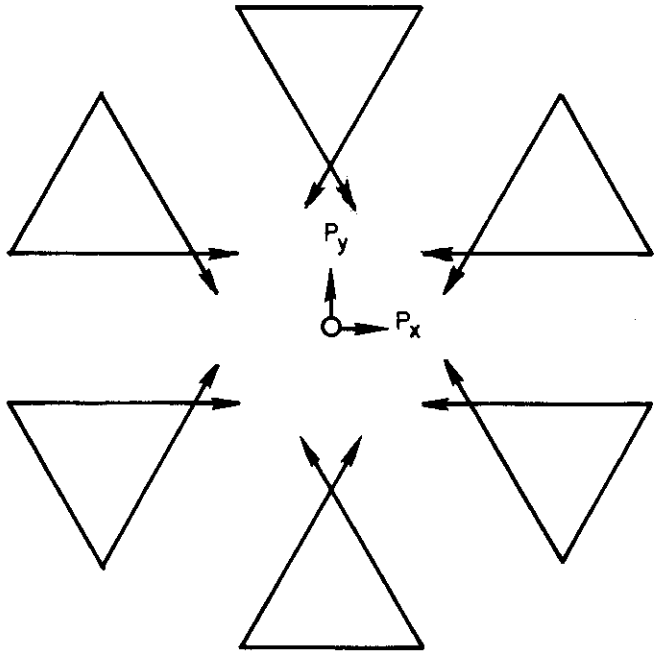

Figure 16. Joint Equilibrium

Figure 16 shows an interior joint of the idealized plate, with the adjoining triangular elements. The external loads P_x and P_y are shown acting on the joint. Also acting on the joint are reactions to the element forces shown acting on the corners of the elements adjacent to the joint. The joint is in equilibirum.

$$\therefore \qquad \left.\begin{aligned} P_x &= -\sum_i F_i \cos \alpha_i \\ P_y &= -\sum_i F_i \sin \alpha_i \end{aligned}\right\} \qquad (17)$$

where the summations include all element forces acting on the joint. Similar equations apply to joints on the edges and corners of the plate.

Equivalent Uniform Stresses

The flexibility matrix Equation 14 is based on the assumption of uniform stress in the panel. The equivalent uniform stresses are given by

$$\begin{bmatrix} \bar{\sigma}_x \\ \bar{\sigma}_y \\ \bar{\tau}_{xy} \end{bmatrix} = \frac{1}{at} \begin{bmatrix} \frac{4\sqrt{3}}{3} & \frac{\sqrt{3}}{3} & \frac{\sqrt{3}}{3} \\ 0 & \sqrt{3} & \sqrt{3} \\ 0 & -1 & 1 \end{bmatrix} \begin{bmatrix} F_1 \\ F_2 \\ F_3 \end{bmatrix} \qquad (18)$$

This transformation is applicable when the edge of the element (or the bar of the equivalent frame) upon which the F_1 force acts is parallel to the x axis.

Linear Stress Field

If the plate is subjected to constant stress, a model composed of constant stress elements yields exact results. A stress distribution one degree more complicated is a distribution in which stresses are linear functions of coordinates. Consider

$$\left.\begin{aligned} \sigma_x &= 2b_3 x + 6b_4 y + 2c_3 \\ \sigma_y &= 6b_1 x + 2b_2 y + 2c_1 \\ \tau_{xy} &= -2b_2 x - 2b_3 y - c_2 \end{aligned}\right\} \qquad (19)$$

These stresses are derived from the stress function

$$\phi = b_1 x^3 + b_2 x^2 y + b_3 xy^2 + b_4 y^3 + c_1 x^2 + c_2 xy + c_3 y^2 \qquad (20)$$

The distribution given by 19 is the most general linear distribution that satisifies equilibrium and the condition $\nabla^4 \phi = 0$. The components of the displacement of a point having the coordinates x and y are given by

$$\left.\begin{aligned} Eu &= -b_1(3\nu x^2 + 3y^2) - b_2(2\nu xy) + b_3(x^2 - 2y^2 - \nu y^2) + b_4(6xy) \\ &\quad - c_1(2\nu x) - c_2(1+\nu)y + c_3(2x) \\ Ev &= b_1(6xy) + b_2(y^2 - 2x^2 - \nu x^2) - b_3(2\nu xy) - b_4(3\nu y^2 + 3x^2) \\ &\quad + c_1(2y) - c_2(1+\nu)x - c_3(2\nu y) \end{aligned}\right\} \qquad (21)$$

Two orientations of the triangular element are considered as shown in Figures 17 and 18. The figures also show the notation for the coordinates of the vertices of the elements. The type II orientation can be derived from the Type I orientation by changing the sign of "a".

Substituting the coordinates of the vertices of the triangles shown in these figures into Equations 21, and setting $\nu = 1/3$ yields expressions for the displacements of the vertices. Substituting these displacements into Equation 15 gives the following expressions for the elongations of the sides of the triangle in the Type I orientation.

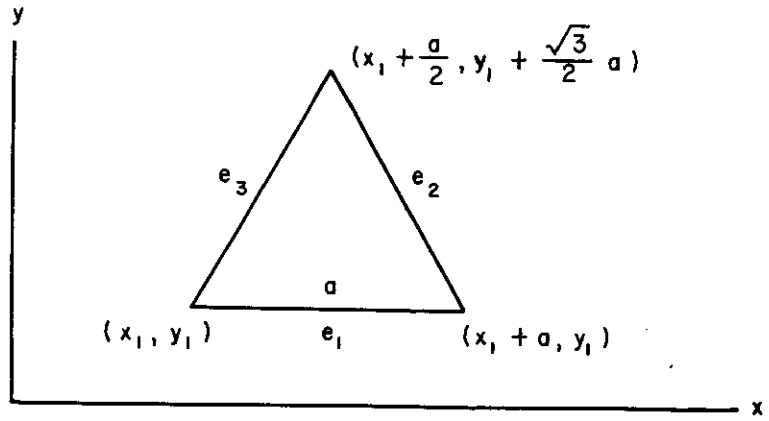

Figure 17. Type I Orientation

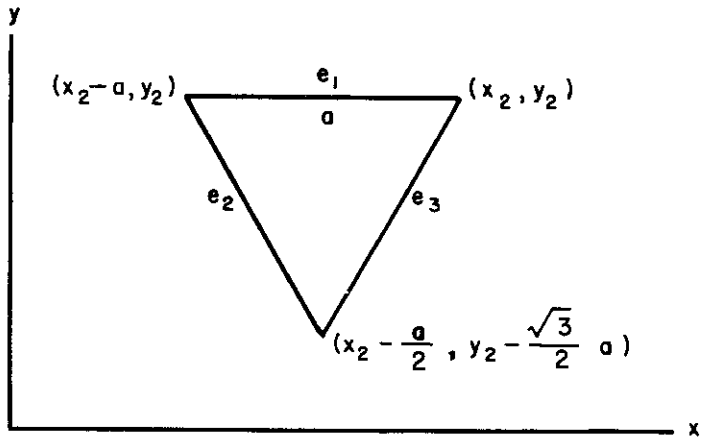

Figure 18. Type II Orientation

$$E\frac{e_1}{a} = b_1(-2x_1 - a) + b_2\left(-\frac{2}{3}y_1\right) + b_3(2x_1 + a) + b_4(6y)_1 + c_1\left(-\frac{2}{3}\right) + c_3(2)$$

$$E\frac{e_2}{a} = b_1(4x_1 + 3a) + b_2\left(\frac{4\sqrt{3}}{3}x_1 + \frac{4}{3}y_1 + \frac{4\sqrt{3}}{3}a\right) + b_3\left(\frac{4\sqrt{3}}{3}y_1 + a\right) + c_1\left(\frac{4}{3}\right) + c_2\left(\frac{2\sqrt{3}}{3}\right) \qquad (22)$$

$$E\frac{e_3}{a} = b_1(4x_1 + a) + b_2\left(-\frac{4\sqrt{3}}{3}x_1 + \frac{4}{3}y_1\right) + b_3\left(-\frac{4\sqrt{3}}{3}y_1 - a\right) + c_1\left(\frac{4}{3}\right) + c_2\left(-\frac{2\sqrt{3}}{3}\right)$$

Expressions for the Type II orientation can be obtained by replacing x_1 by x_2, y_1 by y_2 and a by -a.

External Loads

Eliminating F_i among Equations 16 and 17 gives

$$\left.\begin{aligned} P_x &= -\frac{\sqrt{3}}{4} Et \sum_i e_i \cos \alpha_i \\ P_y &= -\frac{\sqrt{3}}{4} Et \sum_i e_i \sin \alpha_i \end{aligned}\right\} \tag{23}$$

These expressions can be evaluated for an interior joint such as the one shown in Figure 16 by substituting the appropriate element deformations given by Equations 22 or similar expressions applicable to the Type II orientation.

$$\therefore \quad \left.\begin{aligned} P_x &= 0 \\ P_y &= 0 \end{aligned}\right\} \tag{24}$$

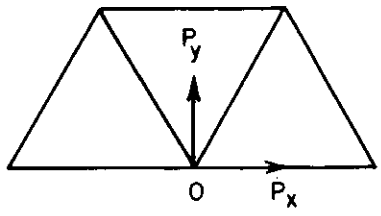

Figure 19. Edge Joint Equilibrium

For an edge joint of the kind shown in Figure 19 the results are

$$\left.\begin{aligned} P_x &= at\,(2b_2 x_0 + 2b_3 y_0 + c_2) \\ P_y &= at\,(-6b_1 x_0 - 2b_2 y_0 - 2c_1) \end{aligned}\right\} \tag{25}$$

where the coordinates of the joint are x_0, y_0.

It can be seen from Equations 25 that P_x and P_y are equal to the shear and normal stresses (with appropriate signs) at the joint multiplied by the length of the element edge and the plate thickness.

This method of establishing idealized normal loads on edge joints appears to neglect couples resulting from the fact that normal edge stresses are linearly distributed rather than constant. Study shows that these couples are exactly balanced by couples acting on other edges that are similarly neglected.

Stresses

Substituting Expressions 22 for e_1, e_2, and e_3 into Equation 16 yields expressions for the element forces F_1, F_2, and F_3. Substituting these expressions into Equation 18 gives the following expressions for the nominal uniform element stresses:

$$\left.\begin{aligned}
\bar{\sigma}_x &= b_2\left(\frac{\sqrt{3}}{3}a\right) + b_3(2x_1 + a) + b_4(6y_1) + c_3(2) \\
\bar{\sigma}_y &= b_1(6x_1 + 3a) + b_2(2y_1 + \sqrt{3}a) + c_1(2) \\
\bar{\tau}_{xy} &= b_1\left(-\frac{\sqrt{3}}{2}a\right) + b_2(-2x_1 - a) + b_3\left(-2y_1 - \frac{\sqrt{3}}{2}a\right) + c_2(-1)
\end{aligned}\right\} \qquad (26)$$

Subtracting the nominal stresses from the true stresses given by Equations 19 and substituting $s = (x - x_1)/a$ and $t = (y - y_1)/a$ leads to the following matrix equation for stress errors:

$$\frac{1}{a}\begin{bmatrix}\Delta\sigma_x \\ \Delta\sigma_y \\ \Delta\tau_{xy}\end{bmatrix} = \left[\begin{array}{c|c} 2b_3 & 6b_4 \\ 6b_1 & 2b_2 \\ -2b_2 & -2b_3 \end{array}\right]\begin{bmatrix}s \\ t\end{bmatrix} + \begin{bmatrix}-\frac{\sqrt{3}}{3}b_2 - b_3 \\ -3b_1 - \sqrt{3}\,b_2 \\ \frac{\sqrt{3}}{2}b_1 + b_2 + \frac{\sqrt{3}}{2}b_3\end{bmatrix} \qquad (27)$$

where $\Delta\sigma_x = \sigma_x - \bar{\sigma}_x$ and $\Delta\sigma_y = \sigma_y - \bar{\sigma}_y$. Let

$$\Delta\boldsymbol{\sigma} = \begin{bmatrix}\Delta\sigma_x \\ \Delta\sigma_y \\ \Delta\tau_{xy}\end{bmatrix};\ \mathbf{A} = \left[\begin{array}{c|c} 2b_3 & 6b_4 \\ 6b_1 & 2b_2 \\ -2b_2 & -2b_3 \end{array}\right];\ \mathbf{S} = \begin{bmatrix}s \\ t\end{bmatrix};\ \mathbf{B} = \begin{bmatrix}-\frac{\sqrt{3}}{3}b_2 - b_3 \\ -3b_1 - \sqrt{3}\,b_2 \\ \frac{\sqrt{3}}{2}b_1 + b_2 + \frac{\sqrt{3}}{2}b_3\end{bmatrix} \qquad (28)$$

$$\therefore \frac{1}{a}\Delta\sigma = AS + B \tag{29}$$

Note that s and t are nondimensional coordinates relative to the element vertex whose coordinates are x_1, y_1. To find a point in the element where the nominal element stresses are equal to the true plate stresses, set $\Delta\sigma = 0$.

$$\therefore AS = -B \tag{30}$$

Unfortunately this matrix equation represents three scalar equations in only two unknowns. Therefore no such point can be found. A point such that $\Delta\sigma_x^2 + \Delta\sigma_y^2 + \Delta\tau_{xy}^2$ is minimized can be found in the following manner:

$$A^T AS = -A^T B \tag{31}$$

$$\therefore \quad S = -(A^T A)^{-1} A^T B \tag{32}$$

Equation 32 was solved for four sets of values of the stress parameters. The results are summarized in Table 1.

TABLE 1

Case	Stress Parameters				Coordinates of Optimum Point		Stress Component Errors		
	b_1	b_2	b_3	b_4	s	t	$\Delta\sigma_x$	$\Delta\sigma_y$	$\Delta\tau_{xy}$
a	1	0	0	0	$\frac{1}{2}$	t	0	0	$\frac{\sqrt{3}}{2}a$
b	0	1	0	0	$\frac{1}{2}$	$\frac{\sqrt{3}}{2}$	$-\frac{\sqrt{3}}{3}a$	0	0
c	0	0	1	0	$\frac{1}{2}$	$\frac{\sqrt{3}}{4}$	0	0	0
d	0	0	0	1	s	0	0	0	0

Stress Errors at the Panel Centroid

The nondimensional coordinates of the panel centroid are s = 1/2, t = $\sqrt{3}/6$. Therefore from Equation 29,

$$\begin{bmatrix} \Delta\sigma_{x_o} \\ \Delta\sigma_{y_o} \\ \Delta\tau_{xy_o} \end{bmatrix} = a \begin{bmatrix} -\frac{\sqrt{3}}{3}b_2 + \sqrt{3}\,b_4 \\ -\frac{2\sqrt{3}}{3}b_2 \\ \frac{\sqrt{3}}{2}b_1 + \frac{\sqrt{3}}{6}b_3 \end{bmatrix} \tag{33}$$

where $\Delta\sigma_{x_o}$, $\Delta\sigma_{y_o}$ and $\Delta\tau_{xy_o}$ are stress errors at the element centroid. These errors are proportional to the length of side of the element and independent of the location of the element.

APPENDIX II

LINEAR STRESS CORRECTION PROCEDURE FOR CONSTANT STRESS MEMBRANE ELEMENTS

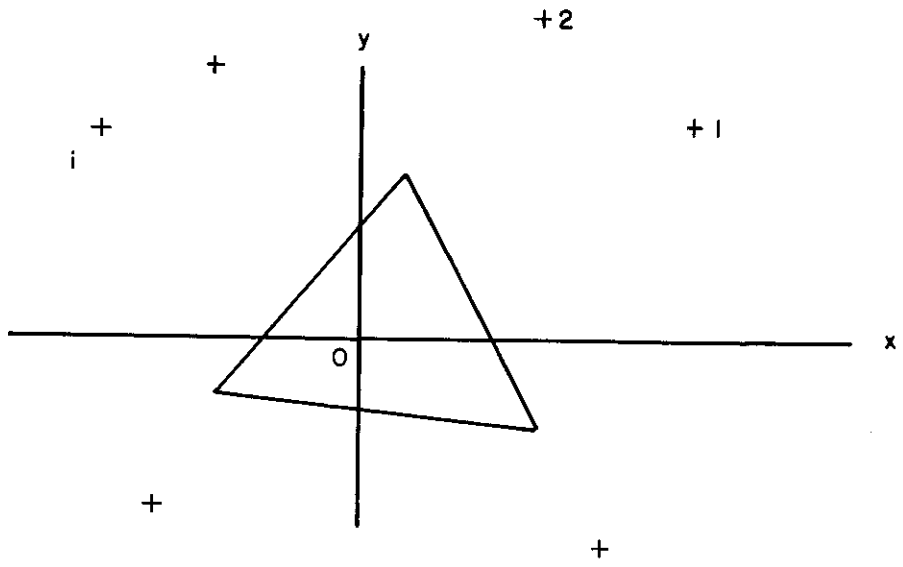

Figure 20. Plate Element

Consider a plate subjected to plane stress. Replace the plate by a model consisting of constant stress elements. Figure 20 shows one such element, not necessarily triangular. Element forces are related to element deformations by

$$F = D^{-1} e \tag{34}$$

where **D** is the flexibility matrix for the element.

Coordinate axes are passed through point 0 as shown. The components of the stress tensor, $\overline{\sigma}_x$, $\overline{\sigma}_y$ and $\overline{\tau}_{xy}$ (constant in the element), are obtained by a transformation of the element forces.

$$\overline{\sigma} = TF \tag{35}$$

where

$$\overline{\sigma} = \begin{bmatrix} \overline{\sigma}_x \\ \overline{\sigma}_y \\ \overline{\tau}_{xy} \end{bmatrix} \tag{36}$$

and **T** is a transformation matrix.

Assume that the idealized plate has been analyzed, so that $\bar{\sigma}$ is known. The nominal stresses $\bar{\sigma}_x$, $\bar{\sigma}_y$ and $\bar{\tau}_{xy}$ are approximations to the components of the true stress tensor at 0. Improved approximations are desired. To obtain such an improvement:

1. Assume that the stress distributions in the plate in the region of the element is approximately linear, so that the components of the stress tensor are given by Equations 19. The corresponding displacements in the region of the element are given by Equations 21.

2. Calculate the deformations of the element resulting from the displacements of Equations 21 in the form

$$e = e_B B + e_C C \tag{37}$$

where

$$B = \begin{bmatrix} b_1 \\ b_2 \\ b_3 \\ b_4 \end{bmatrix} \qquad C = \begin{bmatrix} C_1 \\ C_2 \\ C_3 \end{bmatrix} \tag{38}$$

and e_B and e_C are coefficient matrices whose elements are functions of element geometry.

3. Calculate the element forces from Equation 34 and the nominal stresses from Equation 35.

$$\therefore \quad \bar{\sigma} = \bar{\sigma}_B B + \bar{\sigma}_C C \tag{39}$$

where

$$\bar{\sigma}_B = TD^{-1} e_B \tag{40}$$

and

$$\bar{\sigma}_C = TD^{-1} e_C \tag{41}$$

Let σ_o be a matrix of the true stresses at point 0, i.e.,

$$\sigma_o = \begin{bmatrix} \sigma_{x_o} \\ \sigma_{y_o} \\ \tau_{xy_o} \end{bmatrix} \tag{42}$$

From Equation 19,

$$\sigma_o = \begin{bmatrix} 2c_3 \\ 2c_1 \\ -c_2 \end{bmatrix} \tag{43}$$

If the stresses are constant ($\mathbf{B} = \mathbf{0}$), the nominal stresses in the element given by the matrix $\bar{\sigma}$ must be equal to the true stresses given by the matrix σ_o since the element is a constant stress element. Therefore, from Equation 39

$$\sigma_o = \bar{\sigma}_C \, \mathbf{C} \tag{44}$$

and

$$\sigma_o = \bar{\sigma} - \bar{\sigma}_B \, \mathbf{B} \tag{45}$$

Equation 45 provides a means of correcting the nominal stresses obtained from the use of a constant stress element since it gives the true stresses at the panel center in terms of the nominal stresses. The equation is exact for a linear stress distribution. For a nonlinear distribution the equation will provide an approximate means of correcting the nominal stresses. In the case of a nonlinear distribution the matrix $\mathbf{B}$ can be considered to be a matrix of coefficients of a linear stress field which approximates the nonlinear field in the region of the element. The matrix $\bar{\sigma}_B$ (from Equation 40) is a known function of element geometry and stiffness.

The matrix $\mathbf{B}$ can be established by determining the coefficients b_i so that the stress distribution of Equations 19 approximately reproduces the stresses which have been computed in adjacent elements at points 1, 2 . . . n (Figure 20).

The true stresses at point i can be equated to the linearly distributed stresses of Equations 19.

$$\therefore \quad \begin{bmatrix} \sigma_{x_i} \\ \sigma_{y_i} \\ \tau_{xy_i} \end{bmatrix} = \left[\begin{array}{c|c|c|c} 0 & 0 & 2x_i & 6y_i \\ 6x_i & 2y_i & 0 & 0 \\ 0 & -2x_i & -2y_i & 0 \end{array}\right] \begin{bmatrix} b_1 \\ b_2 \\ b_3 \\ b_4 \end{bmatrix} + \begin{bmatrix} 2c_3 \\ 2c_1 \\ -c_2 \end{bmatrix} \tag{46}$$

$$\therefore \quad \sigma_i = aK_i \, \mathbf{B} + \sigma_o \qquad i = 1, 2 \ldots n \tag{47}$$

where

$$\sigma_i = \begin{bmatrix} \sigma_{x_i} \\ \sigma_{y_i} \\ \tau_{xy_i} \end{bmatrix} \qquad K_i = \frac{1}{a} \begin{bmatrix} 0 & 0 & 2x_i & 6y_i \\ 6x_i & 2y_i & 0 & 0 \\ 0 & -2x_i & -2y_i & 0 \end{bmatrix} \tag{48}$$

and a is a scalar introduced to nondimensionalize the coordinates. The n matrix equations given by Equations 47 can be written

$$\sigma' = a K B + \sigma_0' \tag{49}$$

where

$$\sigma' = \begin{bmatrix} \sigma_1 \\ \sigma_2 \\ \vdots \\ \sigma_n \end{bmatrix}; \quad K = \begin{bmatrix} K_1 \\ K_2 \\ \vdots \\ K_n \end{bmatrix}; \quad \sigma_0' = \begin{bmatrix} \sigma_0 \\ \sigma_0 \\ \vdots \\ \sigma_0 \end{bmatrix} \tag{50}$$

$$\therefore \quad a K B = \sigma' - \sigma_0' \tag{51}$$

Equation 51 represents 3n scalar equations in the unknowns b_1, b_2, b_3 and b_4. The value of n should be at least equal to two, so that Equation 51 involves more scalar equations than unknowns. A linear stress distribution which provides a least squares fit to the true stresses at points 0, 1, 2, . . . n can be obtained as follows:

$$a K^T K B = K^T (\sigma' - \sigma_0') \tag{52}$$

$$B = \frac{1}{a} (K^T K)^{-1} K^T (\sigma' - \sigma_0') \tag{53}$$

Unfortunately the true stresses involved in matrices σ' and σ_0' are not known. A satisfactory approximation to B can be obtained as follows:

$$B = \frac{1}{a} (K^T K)^{-1} K^T (\bar{\sigma}' - \bar{\sigma}_0') \tag{54}$$

where

$$\bar{\sigma}' = \begin{bmatrix} \bar{\sigma} \\ \bar{\sigma}_2 \\ \vdots \\ \bar{\sigma}_n \end{bmatrix} \qquad \bar{\sigma}_0' = \begin{bmatrix} \bar{\sigma}_0 \\ \bar{\sigma}_0 \\ \vdots \\ \bar{\sigma}_0 \end{bmatrix} \tag{55}$$

In other words the coefficients of the linear stress field contained in $\mathbf{B}$ are obtained from the nominal stresses in the elements in the region of point 0. An approximation to the true stress distribution at 0 is then obtained by substituting $\mathbf{B}$ from Equation 54 into Equation 45.

$$\therefore \quad \sigma_0 = \bar{\sigma} + R(\bar{\sigma}' - \bar{\sigma}_0') \tag{56}$$

where

$$R = -\frac{1}{a}\bar{\sigma}_B \, N \tag{57}$$

$$N = (K^T K)^{-1} K^T \tag{58}$$

EQUILATERAL TRIANGULAR GRID

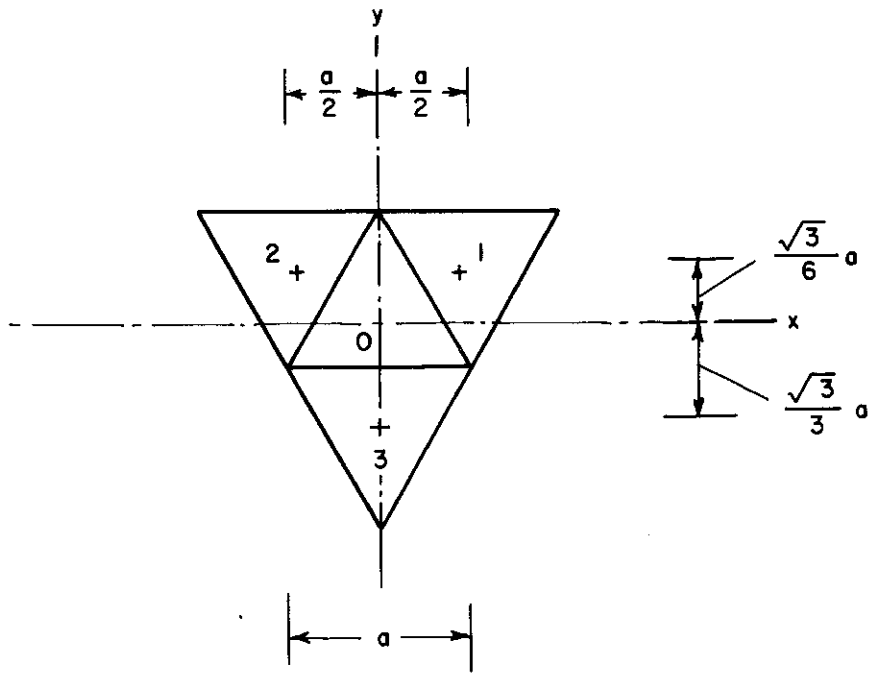

Figure 21. Contiguous Triangular Elements

Figure 21 shows four elements forming part of an equilateral triangular grid. Corrections to the calculated nominal stresses in element "0" are desired based on the assumption that the nominal stresses at points 0, 1, 2 and 3 can be approximated by a linear stress field.

Substituting the coordinates of the four points shown in the figure into the Equation for K (Equation 50) gives:

$$K = \left[\begin{array}{cccc} 0 & 0 & 1 & \sqrt{3} \\ 3 & \frac{\sqrt{3}}{3} & 0 & 0 \\ 0 & -1 & \frac{-\sqrt{3}}{3} & 0 \\ \hline 0 & 0 & -1 & \sqrt{3} \\ -3 & \frac{\sqrt{3}}{3} & 0 & 0 \\ 0 & 1 & \frac{-\sqrt{3}}{3} & 0 \\ \hline 0 & 0 & 0 & -2\sqrt{3} \\ 0 & \frac{-2\sqrt{3}}{3} & 0 & 0 \\ 0 & 0 & \frac{2\sqrt{3}}{3} & 0 \end{array}\right] \qquad (59)$$

$$\therefore \quad K^T K = \begin{bmatrix} 18 & 0 & 0 & 0 \\ 0 & 4 & 0 & 0 \\ 0 & 0 & 4 & 0 \\ 0 & 0 & 0 & 18 \end{bmatrix} \qquad (60)$$

The matrix $K^T K$ is not only nonsingular, but also diagonal.
Substituting K and $K^T K$ into Equation 58 gives:

$$N = \left[\begin{array}{ccc|ccc|ccc} 0 & \frac{1}{6} & 0 & 0 & \frac{-1}{6} & 0 & 0 & 0 & 0 \\ 0 & \frac{\sqrt{3}}{12} & \frac{-1}{4} & 0 & \frac{\sqrt{3}}{12} & \frac{1}{4} & 0 & \frac{-\sqrt{3}}{6} & 0 \\ \frac{1}{4} & 0 & \frac{-\sqrt{3}}{12} & \frac{-1}{4} & 0 & \frac{-\sqrt{3}}{12} & 0 & 0 & \frac{\sqrt{3}}{6} \\ \frac{\sqrt{3}}{18} & 0 & 0 & \frac{\sqrt{3}}{18} & 0 & 0 & \frac{-\sqrt{3}}{9} & 0 & 0 \end{array}\right] \qquad (61)$$

Equation 39 gives the nominal uniform stresses in the triangular element designated "0" in Figure 21. These stresses are given explicitly by Equations 26 for a triangle located as shown in Figure 17. In order to make the coordinate axes of Figure 21 pass through the centroid of the triangle, take $X_1 = -a/2$, $y_1 = -\sqrt{3}a/6$. Equations 26 then become

$$\left.\begin{aligned} \overline{\sigma_x} &= b_2\left(\frac{\sqrt{3}}{3}a\right) + b_4\,(-\sqrt{3}\,a) + c_3\,(2) \\ \overline{\sigma_y} &= b_2\left(\frac{2\sqrt{3}}{3}a\right) + c_1\,(2) \\ \overline{\tau_{xy}} &= b_1\left(-\frac{\sqrt{3}}{2}a\right) + b_3\left(-\frac{\sqrt{3}}{6}a\right) + c_2\,(-1)_1 \end{aligned}\right\} \qquad (62)$$

Comparing Equations 39 and 62 shows that

$$\overline{\sigma}_B = a\begin{bmatrix} 0 & \frac{\sqrt{3}}{3} & 0 & -\sqrt{3} \\ 0 & \frac{2\sqrt{3}}{3} & 0 & 0 \\ \frac{-\sqrt{3}}{2} & 0 & \frac{-\sqrt{3}}{6} & 0 \end{bmatrix} \qquad (63)$$

Substituting **N** and $\overline{\sigma}_B$ from Equations 61 and 63 into Equations 57 gives

$$\mathbf{R} = \begin{bmatrix} \frac{1}{6} & -\frac{1}{12} & \frac{\sqrt{3}}{12} & \frac{1}{6} & -\frac{1}{12} & \frac{\sqrt{3}}{12} & -\frac{1}{3} & \frac{1}{6} & 0 \\ 0 & -\frac{1}{6} & \frac{\sqrt{3}}{6} & 0 & -\frac{1}{6} & \frac{-\sqrt{3}}{6} & 0 & \frac{1}{3} & 0 \\ \frac{\sqrt{3}}{24} & \frac{\sqrt{3}}{12} & \frac{-1}{24} & \frac{-\sqrt{3}}{24} & \frac{-\sqrt{3}}{12} & \frac{-1}{24} & 0 & 0 & \frac{1}{12} \end{bmatrix} \qquad (64)$$

APPENDIX III

EVALUATION OF THE RECTANGULAR BAR-PANEL IDEALIZATION

Figure 22 shows the coordinate system for the idealized plate. Figure 23 shows the notation for displacements and strains of a typical set of bars and panels. Denote the joint whose coordinates are x_i, y_j as the ijth joint. In the following definitions the expressions "horizontal" and "vertical," "left" and "right," "above" and "below," refer to directions and relative positions of bars, panels and joints appearing in Figure 23.

Let

u_{ij}, v_{ij} = components of the displacement of the ijth joint.

ϵx_{ij} = the tensile strain of the bar joining the ijth joint and the shear node to the left of this joint.

$\epsilon' x_{ij}$ = the tensile strain of the bar joining the i-1, jth joint and the shear node to the right of this joint.

ϵy_{ij} = the tensile strain of the bar joining the ijth joint and the shear node below this joint.

$\epsilon' y_{ij}$ = the tensile strain of the bar joining the i, j-1st joint and the shear node above this joint.

γ_{ij} = the shear strain of the panel which has as three of its vertices the ijth joint, the i-1, jth joint and the i, j-1st joint.

a_i, b_j = the lengths of the horizontal and vertical edges of this panel.

η_{ij} = the horizontal displacement of the shear node to the left of the ijth joint.

ζ_{ij} = the vertical displacement of the shear node below the ijth joint.

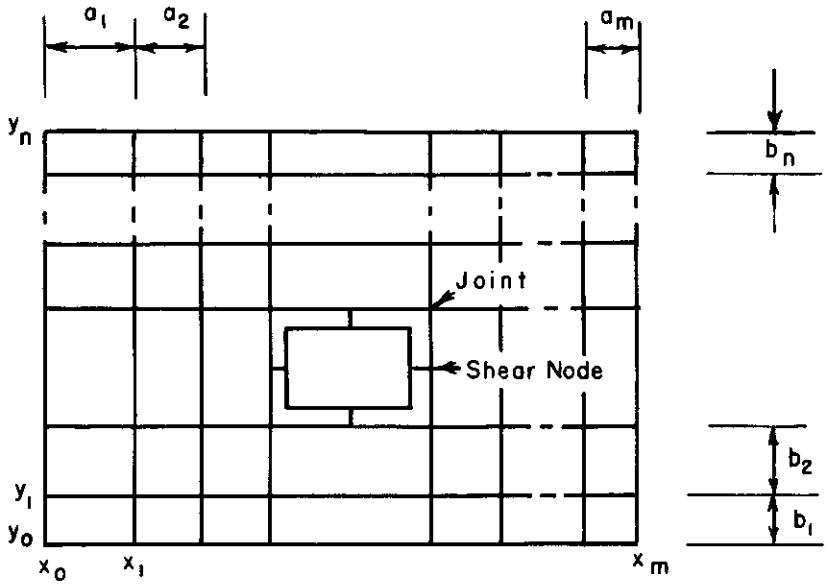

Figure 22. Bar-Panel Idealization

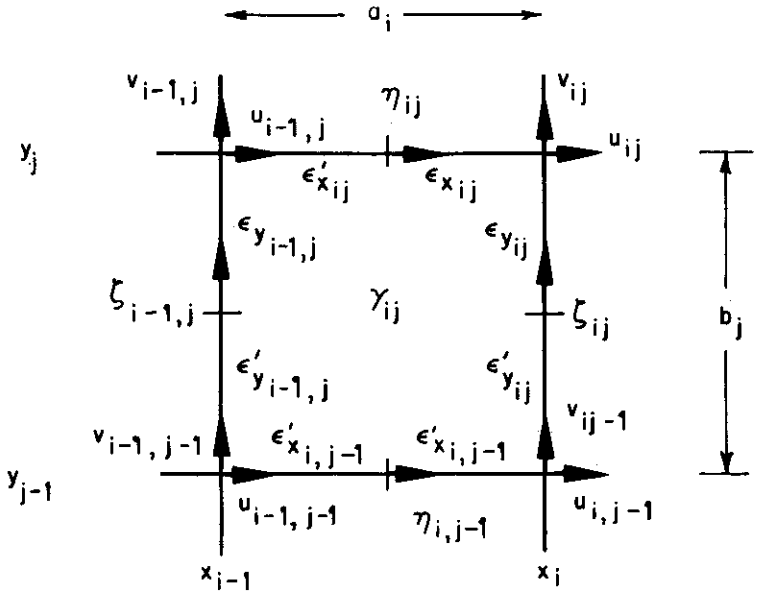

Figure 23. Detail of Bar-Panel Idealization

DIFFERENCE EQUATIONS

Following are the governing equations for the idealized plate:

STRAIN - DISPLACEMENT EQUATIONS

From Figure 23,

$$\epsilon_{x_{ij}} = \frac{2}{a_i}(u_{ij} - \eta_{ij}) \tag{65}$$

$$\epsilon'_{x_{ij}} = \frac{2}{a_i}(\eta_{ij} - u_{i-i,j}) \tag{66}$$

$$\epsilon_{y_{ij}} = \frac{2}{b_j}(v_{ij} - \zeta_{ij}) \tag{67}$$

$$\epsilon'_{y_{ij}} = \frac{2}{b_j}(\zeta_{ij} - v_{i,j-1}) \tag{68}$$

$$\gamma_{xy_{ij}} = \frac{1}{b_j}(\eta_{ij} - \eta_{i,j-1}) + \frac{1}{a_i}(\zeta_{ij} - \zeta_{i-1,j}) \tag{69}$$

STRESS - STRAIN RELATIONSHIPS

$$E\epsilon_{x_{ij}} = \bar{\sigma}_{x_{ij}} - \frac{\nu}{b_j + b_{j+1}}\left(b_j \bar{\sigma}_{y_{ij}} + b_{j+1} \bar{\sigma}'_{y_{i,j+1}}\right) \tag{70}$$

$$E\epsilon'_{x_{i+1,j}} = \bar{\sigma}'_{x_{i+1,j}} - \frac{\nu}{b_j + b_{j+1}}\left(b_j \bar{\sigma}_{y_{ij}} + b_{j+1} \bar{\sigma}'_{y_{i,j+1}}\right) \tag{71}$$

$$E\epsilon_{y_{ij}} = \bar{\sigma}_{y_{ij}} - \frac{\nu}{a_i + a_{i+1}}\left(a_i \bar{\sigma}_{x_{ij}} + a_{j+1} \bar{\sigma}'_{x_{i+1,j}}\right) \tag{72}$$

$$E\epsilon'_{y_{i,j+1}} = \bar{\sigma}'_{y_{i,j+1}} - \frac{\nu}{a_i + a_{i+1}}\left(a_i \bar{\sigma}_{x_{ij}} + a_{i+1} \bar{\sigma}'_{x_{i+1,j}}\right) \tag{73}$$

$$E\gamma_{xy_{ij}} = 2(1+\nu)\bar{\tau}_{xy_{ij}} \tag{74}$$

JOINT EQUILIBRIUM

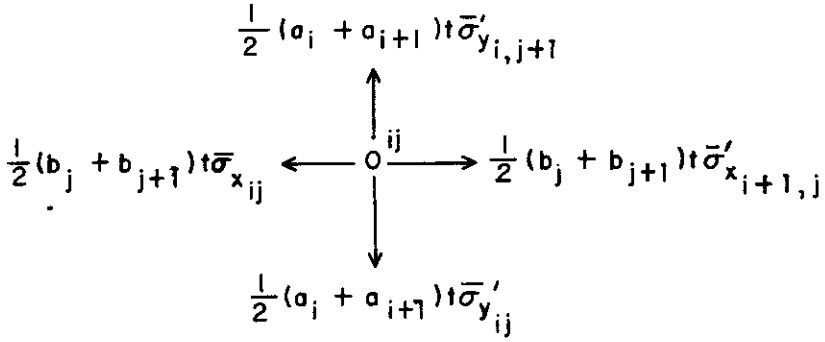

Figure 24. Joint Equilibrium

From Figure 24

$$\bar{\sigma}'_{x_{i+1,\,j}} - \bar{\sigma}_{x_{ij}} = 0 \tag{75}$$

$$\bar{\sigma}'_{y_{i,j+1}} - \bar{\sigma}_{y_{ij}} = 0 \tag{76}$$

SHEAR NODE EQUILIBRIUM

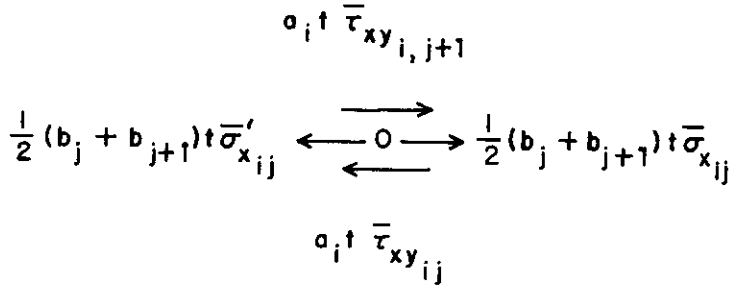

Figure 25. Shear Node Equilibrium

Figure 25 shows the shear node to the left of the ijth joint.

$$\frac{1}{2}(b_j + b_{j+1})\left(\bar{\sigma}_{x_{ij}} - \bar{\sigma}_{x_{i-1,\,j}}\right) + a_i\left(\bar{\tau}_{xy_{i,j+1}} - \bar{\tau}_{xy_{ij}}\right) = 0 \tag{77}$$

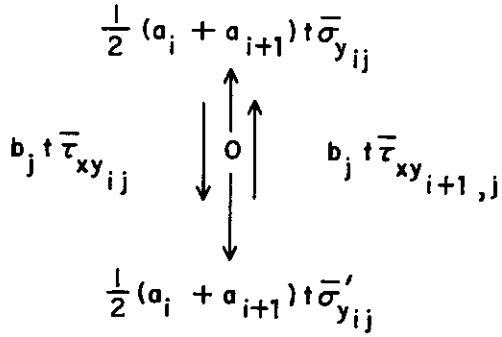

Figuer 26. Shear Node Equilibrium

Figure 26 shows the shear node below the ijth joint.

$$\frac{1}{2}(a_i + a_{i+1})\left(\bar{\sigma}_{y_{ij}} - \bar{\sigma}_{y_{i,j-1}}\right) + b_j\left(\bar{\tau}_{xy_{i+1,j}} - \bar{\tau}_{xy_{ij}}\right) = 0 \tag{78}$$

LINEAR STRESS DISTRIBUTION BOUNDARY CONDITIONS

From Equation 19, neglecting the contribution of the constant stress field:

$$\left.\begin{aligned} \bar{\sigma}_{x_{oj}} &= 2b_3 x_o + 6b_4 y_j \\ \bar{\sigma}'_{x_{m+1,j}} &= 2b_3 x_m + 6b_4 y_j \end{aligned}\right\} \tag{79}$$

$$\left.\begin{aligned} \bar{\sigma}_{y_{io}} &= 6b_1 x_i + 2b_2 y_o \\ \bar{\sigma}'_{y_{i,n+1}} &= 6b_1 x_i + 2b_2 y_n \end{aligned}\right\} \tag{80}$$

$$\left.\begin{aligned} \bar{\tau}_{xy_{oj}} &= -2b_2 x_o - 2b_3\left(y_j - \frac{b_j}{2}\right) \\ \bar{\tau}_{xy_{m+1,j}} &= -2b_2 x_m - 2b_3\left(y_j - \frac{b_j}{2}\right) \\ \bar{\tau}_{xy_{io}} &= -2b_2\left(x_i - \frac{a_i}{2}\right) - 2b_3 y_o \\ \bar{\tau}_{xy_{i,n+1}} &= -2b_2\left(x_i - \frac{a_i}{2}\right) - 2b_3 y_n \end{aligned}\right\} \tag{81}$$

SOLUTION, LINEAR STRESS DISTRIBUTION

The following displacements and stresses satisfy the boundary conditions for the linear stress distribution and the difference equations:

$$\left.\begin{aligned} Eu_{ij} &= -b_1(3\nu x_i^2 + 3y_j^2) - b_2(2\nu x_i y_j) + b_3(x_i^2 - 2y_j^2 - \nu y_j^2) + b_4(6x_i y_j) \\ Ev_{ij} &= b_1(6x_i y_j) + b_2(y_j^2 - 2x_i^2 - \nu x_i^2) - b_3(2\nu x_i y_j) - b_4(3\nu y_j^2 + 3x_i^2) \end{aligned}\right\} \quad (82)$$

$$\left.\begin{aligned} E\eta_{ij} &= -b_1(3\nu x_i^2 + 3y_j^2 - 3\nu a_i x_i) - b_2(2\nu x_i y_j - \nu a_i y_j) \\ &\quad + b_3(x_i^2 - 2y_j^2 - \nu y_j^2 - a_i x_i) + b_4(6x_i y_j - 3a_i y_j) \\ E\zeta_{ij} &= b_1(6x_i y_j - 3b_j x_i) + b_2(y_j^2 - 2x_i^2 - \nu x_i^2 - b_j y_j) \\ &\quad - b_3(2\nu x_i y_j - \nu b_j x_i) - b_4(3\nu y_j^2 + 3x_i^2 - 3\nu b_j y_j) \end{aligned}\right\} \quad (83)$$

$$\left.\begin{aligned} \bar{\sigma}_{x_{ij}} &= 2b_3 x_i + 6b_4 y_j \\ \bar{\sigma}_{y_{ij}} &= 6b_1 x_i + 2b_2 y_j \\ \bar{\tau}_{xy_{ij}} &= -2b_2\left(x_i - \frac{a_i}{2}\right) - 2b_3\left(y_i - \frac{b_j}{2}\right) \end{aligned}\right\} \quad (84)$$

The displacements and stresses given by equations 82 and 84 are in exact agreement with the exact displacements and stresses given by equations 21 and 19, when the results derived from the structural model are interpreted as follows:

1. Joint displacements are equal to displacements of the plate at corresponding points.
2. Bar normal stresses are equal to plate normal stresses at points in the plate corresponding to joints.
3. Panel stresses are equal to plate shear stresses at points in the plate corresponding to panel centers.

Shear node displacements do not match displacements of the plate at corresponding points. These displacements therefore should be disregarded.

QUADRATIC STRESS DISTRIBUTION

The quadratic stress distribution

$$\left.\begin{aligned} \sigma_x &= -d_1(6x^2) + d_4(6xy) - d_5(6x^2 - 12y^2) \\ \sigma_y &= -d_1(6y^2 - 12x^2) + d_2(6xy) - d_5(6y^2) \\ \tau_{xy} &= d_1(12xy) - d_2(3x^2) - d_4(3y^2) + d_5(12xy) \end{aligned}\right\} \quad (85)$$

is derived from the stress function

$$\phi = d_1 x^4 + d_2 x^3 y - 3(d_1 + d_5) x^2 y^2 + d_4 x y^3 + d_5 y^4 \quad (86)$$

The stresses given by Equations 85 satisfy equilibrium and the stress function given by Equation 86 satisfies $\nabla^4 \phi = 0$.

The plate displacements for the case

$$\left.\begin{aligned} &d_1 = 1, d_2 = d_4 = d_5 = 0, \nu = 0 \text{ are} \\ &Eu = -2x^3 \\ &Ev = 12x^2 y - 2y^3 \end{aligned}\right\} \quad (87)$$

The displacements for the case

$$\left.\begin{aligned} &d_2 = 1, d_1 = d_4 = d_5 = 0, \nu = 0 \text{ are} \\ &Eu = -y^3 \\ &Ev = 3xy^2 - 2x^3 \end{aligned}\right\} \quad (88)$$

BOUNDARY CONDITIONS,

$$\left.\begin{aligned} d_1 &= 1, d_2 = d_4 = d_5 = 0 \\ \bar{\sigma}_{x_{oj}} &= -6x_o^2 \\ \bar{\sigma}_{y_{io}} &= 12x_i - 6y_o^2 \\ \bar{\tau}_{xy_{io}} &= 12\left(x_i - \frac{a}{2}\right) y_o \\ \bar{\tau}_{xy_{oj}} &= 12x_o\left(y_i - \frac{b}{2}\right) \end{aligned}\right\} \quad (89)$$

Similar conditions apply to the other boundaries.

SOLUTION, $d_1 = 1$, $d_2 = d_4 = d_5 = 0$.

The following displacements and stresses satisfy the boundary conditions and the difference equations:

$$\left.\begin{aligned} Eu_{ij} &= -2x_i^3 - a^2 x_i \\ Ev_{ij} &= 12x_i^2 y_j - 2y_j^3 - b^2 y_j \end{aligned}\right\} \tag{90}$$

$$\left.\begin{aligned} E\eta_{ij} &= -2x_i^3 + 2ax_i^2 \\ E\zeta_{ij} &= 12x_i^2 y_j - 2y_j^3 - 6bx_i^2 + 3by_j^2 - b^2 y_j \end{aligned}\right\} \tag{91}$$

$$\bar{\sigma}_{\chi_{ij}} = -6x_i^2 \tag{92}$$

$$\bar{\sigma}_{y_{ij}} = 12x_i^2 - 6y_j^2 \tag{93}$$

$$\bar{\tau}_{xy_{ij}} = 12\left(x_i - \frac{a}{2}\right)\left(y_j - \frac{b}{2}\right) \tag{94}$$

The errors obtained by comparing these solutions with the exact equations are as follows:

$$\left.\begin{aligned} E\Delta u_{ij} &= -a^2 x_i \\ E\Delta v_{ij} &= -b^2 y_j \end{aligned}\right\} \tag{95}$$

$$\Delta\sigma_{x_{ij}} = \Delta\sigma_{y_{ij}} = \Delta\tau_{xy_{ij}} = 0 \tag{96}$$

BOUNDARY CONDITIONS, $d_2 = 1$, $d_1 = d_4 = d_5 = 0$

$$\left.\begin{aligned} \bar{\sigma}_{\chi_{oj}} &= 0 \\ \bar{\sigma}_{y_{io}} &= 6x_i y_o \\ \bar{\tau}_{xy_{io}} &= -3x_i^2 + 3x_i a - a^2 \\ \bar{\tau}_{xy_{oj}} &= -3x_o^2 - a^2 \end{aligned}\right\} \tag{97}$$

The shear stress $\bar{\tau}_{xy_{io}}$ represents the average shear stress at the shear node on the lower edge of the structural model between the joint at $x_{i-1,0}$ and the joint at x_{io}. The shear stress $\bar{\tau}_{xy_{oj}}$ equals a contribution $(-3x_o^2)$ representing the constant shear stress on the left hand edge of the model and a contribution $(-a^2)$ necessary to provide equilibrium of moments on the model. Similar conditions apply to the other boundaries.

SOLUTION, $d_2 = 1$, $d_1 = d_4 = d_5 = 0$

The following displacements and stresses satisfy the boundary conditions and the difference equations:

$$\left.\begin{aligned} Eu_{ij} &= -y_j^3 \\ Ev_{ij} &= 3x_i y_j^2 - 2x_i^3 + b^2 x_i \end{aligned}\right\} \tag{98}$$

$$\left.\begin{aligned} E\eta_{ij} &= -y_j^3 \\ E\zeta_{ij} &= 3x_i y_j (y_j - b) - 2x_i^3 + b^2 x_i^2 \end{aligned}\right\} \tag{99}$$

$$\left.\begin{aligned} \bar{\sigma}_{x_{ij}} &= 0 \\ \bar{\sigma}_{y_{ij}} &= 6x_i y_j \\ \bar{\tau}_{xy_{ij}} &= -3\left(x_i - \frac{a}{2}\right)^2 - \frac{a^2}{4} \end{aligned}\right\} \tag{100}$$

The errors are as follows:

$$\left.\begin{aligned} E\Delta u &= 0 \\ E\Delta v &= b^2 x_i^2 \end{aligned}\right\} \tag{101}$$

$$\left.\begin{aligned} \Delta\sigma_x = \Delta\sigma_y &= 0 \\ \Delta\tau_{xy} &= -\frac{a^2}{4} \end{aligned}\right\} \tag{102}$$

APPENDIX IX

STEADY STATE VIBRATION OF DAMPED ELASTIC STRUCTURES

Equations are presented for the analysis of steady state vibrations of damped elastic structures by the Matrix Displacement, Matrix Force, and Unified methods.

GOVERNING EQUATIONS

Dynamic Equilibrium:

$$P_E F_E + P_D F_D + P_m F_m + P_R R + P_\phi \phi = 0 \tag{103}$$

where P_E, P_D, P_m, P_R and P_ϕ are rectangular matrices of components in the joint degrees of freedom of unit values of elastic element forces, damping element forces, inertia force components, reactions and external loads, and F_E, F_D, F_m, R and ϕ are column matrices of elastic element forces, damping element forces, inertia forces, reactions and external loads. The later group of matrices are time dependent. This equation can also be written as follows:

$$P_{UE} F_E + P_{UD} F_D + P_{Um} F_m + P_{UR} R + P_{U\phi} \phi = 0 \tag{104}$$

$$P_{CE} F_E + P_{CD} F_D + P_{Cm} F_m + P_{CR} R + P_{C\phi} \phi = 0 \tag{105}$$

where P_{UE}, P_{UD}, P_{Um}, P_{UR} and $P_{U\phi}$ are components in the unconstrained joint degrees of freedom of unit values of the elastic element forces, the damping element forces, the inertia forces and the external loads, and P_{CE}, P_{CD}, P_{Cm}, P_{CR} and $P_{C\phi}$ are corresponding matrices for the constrained joint degrees of freedom. The unconstrained joint degrees of freedom are selected in such a manner that reactions have no components in these degrees of freedom.

$$\therefore \quad P_{UR} = 0 \tag{106}$$

FORCE-DEFORMATION EQUATIONS

$$F_E = k e_E \tag{107}$$

$$F_D = c \dot{e}_D \tag{108}$$

$$F_m \quad m \ddot{\Delta}_m \tag{109}$$

where $\mathbf{k}$, $\mathbf{c}$ and $\mathbf{m}$ are square matrices of element stiffnesses, damping constants and masses and $\mathbf{e}_E$, $\mathbf{e}_D$ and Δ_m are column matrices of elastic element deformations, damping element deformations and joint displacement components, respectively.

EQUATIONS OF COMPATIBILITY

The following equations can be derived from the principle of virtual work:

$$\mathbf{e}_E + \mathbf{e}_A = -P_{UE}^T \Delta - P_{CE}^T \Delta_R \tag{110}$$

$$\mathbf{e}_D + \mathbf{e}_B = -P_{UD}^T \Delta - P_{CD}^T \Delta_R \tag{111}$$

$$\Delta_m + \mathbf{e}_m = -P_{Um}^T \Delta - P_{Cm}^T \Delta_R \tag{112}$$

where Δ and Δ_R are column matrices of components of joint displacements in the unconstrained and constrained degrees of freedom respectively and $\mathbf{e}_A$ and $\mathbf{e}_B$ are column matrices of unassembled deformations of the elastic and damping elements respectively. The matrix $\mathbf{e}_m$ is defined subsequently.

SINUSOIDAL EXCITATION, STEADY STATE RESPONSE

Equations 104 to 112 inclusive are the governing equations for the structure subjected to arbitrary time varying external loads, support displacements and unassembled deformations. Assume that these forcing functions are sinusoidal functions of time of a single frequency ω but varying phase. Any such function Y can be written in the form

$$Y = Y_s \sin \omega t + Y_c \cos \omega t \tag{113}$$

where $Y_s = |Y| \cos \theta_y$, $Y_c = |Y| \sin \theta_y$, $|Y|$ is the amplitude of the forcing function and θ_y is the phase angle. A sufficiently long time after the initiation of the dynamic process all structural responses are sinusoidal functions of the time of frequency ω. Each response therefore can be written in the form of equation 113. In the following the quantities Y_s and Y_c are called the sine and cosine components of Y. Sine and cosine components are denoted by adding subscripts S and T respectively to the symbol for a forcing function or response. For example, the matrix of unconstrained displacement components is written

$$\Delta = \Delta_s \sin \omega t + \Delta_c \cos \omega t \tag{114}$$

UNIFIED MATRIX METHOD

Substitute expressions of the form of equation 114 for F_E, F_D, F_m and ϕ into equation 104. Equating like terms yields

$$\left.\begin{aligned} P_U\ F_S + P_{U\phi}\phi_S &= 0 \\ P_U\ F_C + P_{U\phi}\phi_C &= 0 \end{aligned}\right\} \tag{115}$$

where

$$P_U = \left[\, P_{UE}\ P_{Um}\ P_{UD} \right] \tag{116}$$

$$F_S = \left\{ F_{ES}\ F_{mS}\ F_{DS} \right\} \qquad F_C = \left\{ F_{EC}\ F_{mC}\ F_{DC} \right\} \tag{117}$$

and the symbols $[\ ]$ and $\{\ \}$ denote rectangular and column matrices, respectively.

In a similar manner Equations 107, 108 and 109 yield

$$\left.\begin{aligned} F_S &= \eta e_S - \zeta e_C \\ F_C &= \zeta e_S + \eta e_C \end{aligned}\right\} \tag{118}$$

where

$$\eta = \begin{bmatrix} k & & \\ & -\omega^2 m & \\ & & 0 \end{bmatrix} \qquad \zeta = \begin{bmatrix} 0 & & \\ & 0 & \\ & & \omega c \end{bmatrix} \tag{119}$$

$$e_S = \left\{ e_{ES}\ \Delta_{mS}\ e_{DS} \right\} \qquad e_C = \left\{ e_{EC}\ \Delta_{mC}\ e_{DC} \right\} \tag{120}$$

Similarly Equations 110, 111 and 112 can be written

$$\left.\begin{aligned} e_S + e_{TS} &= -P_U^T\ \Delta_S - P_C^T \Delta_{RS} \\ e_C + e_{TC} &= -P_U^T\ \Delta_C - P_C^T \Delta_{RC} \end{aligned}\right\} \tag{121}$$

where

$$e_{TS} = \left\{ e_{AS}\ e_{mS}\ e_{BS} \right\} \qquad e_{TC} = \left\{ e_{AC}\ e_{mC}\ e_{BC} \right\} \tag{122}$$

$$P_C = \left[\, P_{CE}\ P_{Cm}\ P_{CD} \right] \tag{123}$$

Let

$$\eta^* = \begin{bmatrix} k^{-1} & & \\ & -\frac{m^{-1}}{\omega^2} & \\ & & 0 \end{bmatrix} \qquad \zeta^* = \begin{bmatrix} 0 & & \\ & 0 & \\ & & \frac{c^{-1}}{\omega} \end{bmatrix} \tag{124}$$

$$\text{Note that } \eta^*\eta + \zeta^*\zeta = I \qquad \eta^*\zeta = \zeta^*\eta = 0 \tag{125}$$

Solving equation 118 for e_S and e_C and substituting the results into Equation 121 yields

$$\left.\begin{aligned} \eta^* F_S + \zeta^* F_C + P_U^T \Delta_S + e_{TS} + P_C^T \Delta_{RS} &= 0 \\ -\zeta^* F_S + \eta^* F_C + P_U^T \Delta_C + e_{TC} + P_C^T \Delta_{RC} &= 0 \end{aligned}\right\} \tag{126}$$

Equations 115 and 126 can be written as follows:

$$\begin{bmatrix} \eta^* & \zeta^* & P_U^T & 0 \\ -\zeta^* & \eta^* & 0 & P_U^T \\ P_U & 0 & 0 & 0 \\ 0 & P_U & 0 & 0 \end{bmatrix} \begin{bmatrix} F_S \\ F_C \\ \Delta_S \\ \Delta_C \end{bmatrix} + \begin{bmatrix} e_{TS} + P_C^T \Delta_{RS} \\ e_{tc} + P_C^T \Delta_{RC} \\ P_{U\phi}\phi_S \\ P_{U\phi}\phi_C \end{bmatrix} = 0 \tag{127}$$

Equation 127 is the Unified Matrix equation for steady state damped structural vibration. The equation can be solved for the sine and cosine components of the element forces and displacements.

ELASTIC ANALOGY

The structure can be replaced by an analogous structure in which the masses are replaced by negative springs. Equations 119 show that the unassembled stiffness matrix for these negative springs is $-\omega^2 m$.

Equation 120 shows that the negative spring deformations are equal to the joint displacements. The negative springs therefore must be considered to be attached to the frame of reference. Equations 122 show that e_{mS} and e_{mC} are sine and cosine components of unassembled deformations of the negative springs.

MATRIX DISPLACEMENT METHOD

Solving Equations 121 for $\mathbf{e}_S$ and $\mathbf{e}_C$ and substituting the results into Equations 118 yields

$$\left.\begin{aligned} \mathbf{F}_s &= -\eta \mathbf{P}_U^T \Delta_S + \zeta \mathbf{P}_U^T \Delta_C - \eta \mathbf{e}_{TS} + \zeta \mathbf{e}_{TC} - \eta \mathbf{P}_C^T \Delta_{RS} + \zeta \mathbf{P}_C^T \Delta_{RC} \\ \mathbf{F}_c &= -\zeta \mathbf{P}_U^T \Delta_S - \eta \mathbf{P}_U^T \Delta_C - \zeta \mathbf{e}_{TS} - \eta \mathbf{e}_{TC} - \zeta \mathbf{P}_C^T \Delta_{RS} - \eta \mathbf{P}_c^T \Delta_{RC} \end{aligned}\right\} \quad (128)$$

Substituting $\mathbf{F}_S$ and $\mathbf{F}_C$ from Equations 128 into Equations 115 yields

$$\left.\begin{bmatrix} \mathbf{S} & -\mathbf{T} \\ \mathbf{T} & \mathbf{S} \end{bmatrix} \begin{bmatrix} \Delta_S \\ \Delta_C \end{bmatrix} = \begin{bmatrix} \psi_S \\ \psi_C \end{bmatrix}\right\} \quad (129)$$

where

$$\left.\begin{aligned} \psi_S &= \mathbf{P}_U \phi \phi_S - \mathbf{P}_U \eta \mathbf{e}_{TS} + \mathbf{P}_U \zeta \mathbf{e}_{TC} - \mathbf{S}_{UC} \Delta_{RS} + \mathbf{T}_{RC} \Delta_{RC} \\ \psi_C &= \mathbf{P}_U \phi \phi_C - \mathbf{P}_U \zeta \mathbf{e}_{TS} - \mathbf{P}_U \eta \mathbf{e}_{TC} - \mathbf{T}_{UC} \Delta_{RS} - \mathbf{S}_{UC} \Delta_{RC} \end{aligned}\right\} \quad (130)$$

$$\left.\begin{aligned} \mathbf{S} &= \mathbf{P}_U \eta \mathbf{P}_U^T \qquad \mathbf{T} = \mathbf{P}_U \zeta \mathbf{P}_U^T \\ \mathbf{S}_{UC} &= \mathbf{P}_U \eta \mathbf{P}_C^T \qquad \mathbf{T}_{UC} = \mathbf{P}_U \zeta \mathbf{P}_C^T \end{aligned}\right\} \quad (131)$$

Equation 129 can be solved for the sine and cosine components of displacements by three methods. Two of these methods involve finding $\mathbf{S}^{-1}$ or $\mathbf{T}^{-1}$ or solving the equations by equivalent procedures. The method which involves $\mathbf{S}^{-1}$ is likely to be inaccurate in the case of a complicated structure having many natural frequencies because $\mathbf{S}$ is poorly conditioned when the impressed frequency is close to a natural frequency. The matrix $\mathbf{T}$ is likely to be poorly conditioned or singular if some of the structural elements have zero damping. The third and best procedure involves solving the complete set of equations by elimination, employing a pivot selection technique. Element forces can be calculated from Equations 128.

Equations 128 and 129 are the Matrix Displacement equations for damped structural vibration.

MATRIX FORCE METHOD

The restriction that reactions have no components in the unconstrained degrees of freedom is removed. Equation 103 can be written

$$\mathbf{P}_{FR} \mathbf{F}_R + \mathbf{P}_\phi \phi = 0 \quad (132)$$

where

$$P_{FR} = \left[P_E \quad P_m \quad P_D \quad P_R \right] \quad F_R = \left\{ F_E \quad F_m \quad F_D \quad R \right\} \tag{133}$$

The element forces can be expressed in terms of the redundants and the external loads as

$$F_R = f_X X + f_\phi \phi \tag{134}$$

where f_X and f_ϕ are rectangular matrices of element forces resulting from unit values of the redundants and of the external loads respectively, and X is a column matrix of redundants. Note that the negative springs representing the masses are considered part of the structure. The forces in these negative springs can be selected as redundants. The matrices f_X and f_ϕ are independent of time; they can be computed from P_F and P_ϕ through procedures applicable to static analysis.

The sine and cosine components of F_R are obtained by substituting expressions of the form of Equation 114 for F, X and ϕ into Equation 134 to yield

$$\left.\begin{aligned} F_{RS} &= f_X X_S + f_\phi \phi_S \\ F_{RC} &= f_X X_C + f_\phi \phi_C \end{aligned}\right\} \tag{135}$$

The compatibility conditions (Equations 126) can be written

$$\left.\begin{aligned} \eta^*_{FR} F_{RS} + \zeta^*_{FR} F_{RC} + P^T_{FR} \Delta_{UCS} + e_{FRS} &= 0 \\ -\zeta^*_{FR} F_{RS} + \eta^*_{FR} F_{RC} + P^T_{FR} \Delta_{UCC} + e_{FRC} &= 0 \end{aligned}\right\} \tag{136}$$

where

$$\eta^*_{FR} = \begin{bmatrix} \eta^* & \\ & 0 \end{bmatrix} \qquad \zeta^*_{FR} = \begin{bmatrix} \zeta^* & \\ & 0 \end{bmatrix} \tag{137}$$

$$\Delta_{UCS} = \left\{ \Delta_S \quad \Delta_{RS} \right\} \qquad \Delta_{UCC} = \left\{ \Delta_C \quad \Delta_{RC} \right\} \tag{138}$$

$$e_{FRS} = \left\{ e_{TS} - \Delta_{rS} \right\} \qquad e_{FRC} = \left\{ e_{TC} - \Delta_{rC} \right\} \tag{139}$$

and Δ_r is a matrix of reaction displacements.

Substituting F_{RS} and F_{RC} from equations 135 into equations 136 and multiplying both equations through by f_X^T gives

$$\delta_{XX} x_S + \bar{\delta}_{XX} x_C + \delta_{X\phi} \phi_S + \bar{\delta}_{X\phi} \phi_C + (P_{FR} f_X)^T \Delta_{UCS} + f_X^T \bullet_{FRS} = 0 \tag{140}$$

$$-\bar{\delta}_{XX} x_S + \delta_{XX} x_C - \bar{\delta}_{X\phi} \phi_X + \delta_{X\phi} \phi_C + (P_{FR} f_X)^T \Delta_{UCC} + f_X^T \bullet_{FRC} = 0 \tag{141}$$

where

$$\delta_{XX} = f_X^T \eta_{FR}^* f_X \qquad \bar{\delta}_{XX} = f_X^T \zeta_{FR}^* f_X \tag{142}$$

$$\delta_{X\phi} = f_X^T \eta_{FR}^* f_\phi \qquad \bar{\delta}_{X\phi} = f_X^T \zeta_{FR}^* f_\phi \tag{143}$$

The matrix $P_{FR} f_X$ can be shown to be null. Therefore

$$\begin{bmatrix} \delta_{XX} & \bar{\delta}_{XX} \\ \bar{\delta}_{XX} & \delta_{XX} \end{bmatrix} \begin{bmatrix} x_S \\ x_C \end{bmatrix} = \begin{bmatrix} \lambda_S \\ \lambda_C \end{bmatrix} \tag{144}$$

where

$$\left.\begin{aligned} \lambda_S &= -\delta_{X\phi} \phi_S - \bar{\delta}_{X\phi} \phi_C - f_X^T \bullet_{FRS} \\ \lambda_C &= \bar{\delta}_{X\phi} \phi_S - \delta_{X\phi} \phi_C - f_X^T \bullet_{FRC} \end{aligned}\right\} \tag{145}$$

Equations 144 can be solved for the sine and cosine components of the redundants. As in the Displacement Method the best approach appears to be to solve the complete set of equations by elimination, employing a pivot selection technique. Element forces can be calculated from Equation 135. Deflections can be obtained by calculating the deformations of the negative springs as follows:

$$\left.\begin{aligned} \Delta_S &= \frac{1}{\omega^2} P_{Um} m^{-1} F_{mS} - P_{Um} \bullet_{mS} \\ \Delta_C &= \frac{1}{\omega^2} P_{Um} m^{-1} F_{mC} - P_{Um} \bullet_{mC} \end{aligned}\right\} \tag{146}$$

Equations 135, 144, and 146 are the Matrix Force equations for steady state damped structural vibration.